UCSF
UC San Francisco Previously Published Works

Title

SCUBE1 Controls BMPR2-Relevant Pulmonary Endothelial Function Implications for Diagnostic Marker Development in Pulmonary Arterial Hypertension

Permalink

https://escholarship.org/uc/item/2pr071fz

Journal

JACC Basic to Translational Science, 5(11)

ISSN

2452-302X

Authors

Sun, Wei
Tang, Ying
Tai, Yi-Yin
et al.

Publication Date

2020-11-01

DOI

10.1016/j.jacbts.2020.08.010

Peer reviewed

eScholarship.org Powered by the California Digital Library
University of California

JACC: BASIC TO TRANSLATIONAL SCIENCE
PUBLISHED BY ELSEVIER ON BEHALF OF THE AMERICAN COLLEGE OF CARDIOLOGY FOUNDATION. THIS IS AN OPEN ACCESS ARTICLE UNDER THE CC BY-NC-ND LICENSE (http://creativecommons.org/licenses/by-nc-nd/4.0/).

VOL. 5, NO. 11, 2020

PRECLINICAL RESEARCH

SCUBE1 Controls BMPR2-Relevant Pulmonary Endothelial Function

Implications for Diagnostic Marker Development in Pulmonary Arterial Hypertension

Wei Sun, MD,[a] Ying Tang, MS,[a] Yi-Yin Tai, MS,[a] Adam Handen, MS,[a] Jingsi Zhao, MS,[a] Gil Speyer, PHD,[b] Yassmin Al Aaraj, MD,[a] Annie Watson, MPH,[a] Makenna E. Romanelli,[a] John Sembrat, BS,[a] Mauricio Rojas, MD,[a] Marc A. Simon, MD,[a] Yingze Zhang, PHD,[a] Janet Lee, MD,[a] Zeyu Xiong, MD, MS,[a] Partha Dutta, DVM, PHD,[a] Sathish Badu Vasamsetti, PHD,[a] Dennis McNamara, MD,[a] Bryan McVerry, MD,[a] Charles F. McTiernan, PHD,[a] Frank C. Sciurba, MD,[a] Seungchan Kim, PHD,[c] Kerri Akaya Smith, MD,[d] Jeremy A. Mazurek, MD,[e] Yuchi Han, MD,[e] Anjali Vaidya, MD,[f] Seyed Mehdi Nouraie, MD, PHD,[a] Neil J. Kelly, MD,[a] Stephen Y. Chan, MD, PHD[a]

VISUAL ABSTRACT

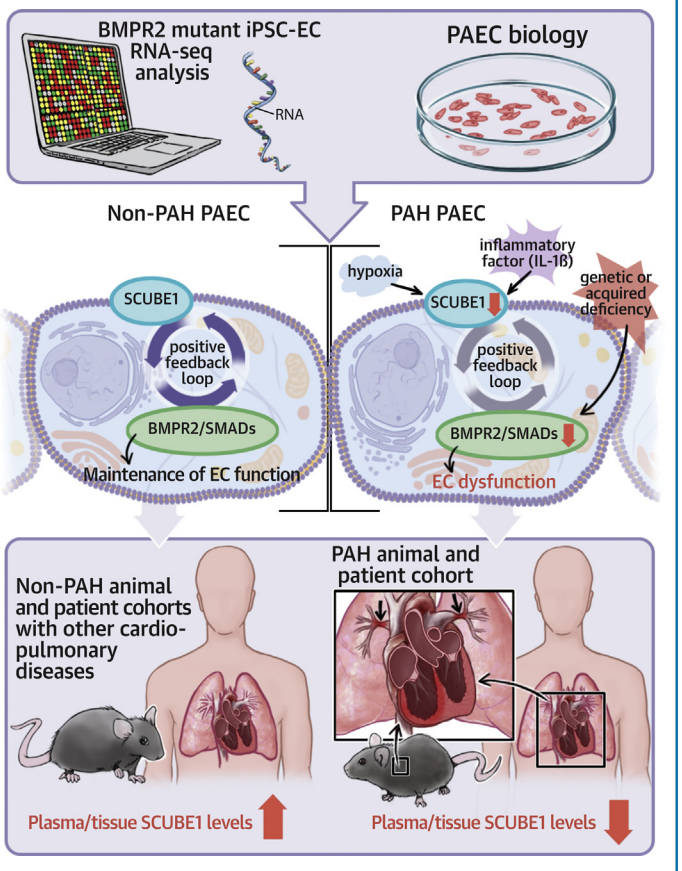

Sun, W. et al. J Am Coll Cardiol Basic Trans Science. 2020;5(11):1073–92.

ISSN 2452-302X

https://doi.org/10.1016/j.jacbts.2020.08.010

ABBREVIATIONS AND ACRONYMS

BMP = bone morphogenetic protein

EC = endothelial cell

iPSC-EC = induced pluripotent stem cell-endothelial cell

mPAP = mean pulmonary artery pressure

PAEC = pulmonary arterial endothelial cell

PAH = pulmonary arterial hypertension

PAP = pulmonary artery pressure

PCWP = pulmonary capillary wedge pressure

PH = pulmonary hypertension

PVR = pulmonary vascular resistance

RV = right ventricle

WSPH = World Symposium on Pulmonary Hypertension

HIGHLIGHTS

- **Guided by public sequencing data of iPSC-derived BMPR2-mutant ECs derived from patients with PAH and related family members, SCUBE1 was found to be differentially expressed in ECs carrying BMPR2 mutations, dependent on HIF1A and down-regulated by PAH triggers.**
- **SCUBE1 deficiency controlled BMPR2-associated SMAD1/5/9 signaling, thus regulating endothelial angiogenic potential, proliferation, and apoptosis.**
- **SCUBE1 was decreased specifically in plasma and lungs in rodents and patients with PAH but not in those with PH due to left heart disease or other acute or chronic pulmonary and cardiovascular diseases.**
- **A plasma SCUBE1 cutpoint of 5.46 ng/ml was defined to distinguish PAH from non-PAH contexts, with a high specificity (0.87) and a significant diagnostic OR (7.6).**
- **In PAH patients, plasma SCUBE1 levels negatively correlated with PA pressure, pulmonary vascular resistance, and RV dysfunction.**
- **These findings support the notion of SCUBE1 as a clinical biomarker of PAH, reflecting the severity and progression of PAH and inherently linked to disease pathogenesis and genetic predisposition.**

SUMMARY

Utilizing publicly available ribonucleic acid sequencing data, we identified *SCUBE1* as a BMPR2-related gene differentially expressed between induced pluripotent stem cell-endothelial cells derived from pulmonary arterial hypertension (PAH) patients carrying pathogenic BMPR2 mutations and control patients without mutations. Endothelial SCUBE1 expression was decreased by known triggers of PAH, and its down-regulation recapitulated known BMPR2-associated endothelial pathophenotypes in vitro. Meanwhile, SCUBE1 concentrations were reduced in plasma obtained from PAH rodent models and patients with PAH, whereas plasma concentrations were tightly correlated with hemodynamic markers of disease severity. Taken together, these data implicate SCUBE1 as a novel contributor to PAH pathogenesis with potential therapeutic, diagnostic, and prognostic applications. (J Am Coll Cardiol Basic Trans Science 2020;5:1073–92) Published by Elsevier on behalf of the American College of Cardiology Foundation. This is an open access article under the CC BY-NC-ND license (http://creativecommons.org/licenses/by-nc-nd/4.0/).

Pulmonary hypertension (PH) and its particularly severe subtype pulmonary arterial hypertension (PAH) are highly morbid diseases. These conditions are pathologically characterized by progressive pulmonary vascular remodeling and obliteration of pulmonary arterioles, resulting in significantly increased pulmonary vascular resistance (PVR) and pulmonary arterial pressure (PAP) (1). The elevated PAP and PVR increase right heart afterload leading to progressive right ventricular (RV) hypertrophy, dilation, and failure over time (2). World Symposium on Pulmonary Hypertension (WSPH) group 1 PAH is composed of idiopathic, heritable, and comorbid etiologies, such as connective tissue disorders, infections, and others. In particular, pathogenic mutations

From the [a]Center for Pulmonary Vascular Biology and Medicine, Pittsburgh Heart, Lung, Blood, and Vascular Medicine Institute, Division of Cardiology and Division of Pulmonary, Allergy, and Critical Care Medicine, Department of Medicine, University of Pittsburgh School of Medicine and University of Pittsburgh Medical Center, Pittsburgh, Pennsylvania, USA; [b]Research Computing, Arizona State University, Tempe, Arizona, USA; [c]Center for Computational Systems Biology, Department of Electrical and Computer Engineering, Roy G. Perry College of Engineering, Prairie View A and M University, Prairie View, Texas, USA; [d]Division of Pulmonary Medicine, Perelman School of Medicine, University of Pennsylvania, Philadelphia, Pennsylvania, USA; [e]Division of Cardiovascular Medicine, Perelman School of Medicine, University of Pennsylvania, Philadelphia, Pennsylvania, USA; and the [f]Cardiovascular Division, Temple University Health Systems, Philadelphia, Pennsylvania, USA.

The authors attest they are in compliance with human studies committees and animal welfare regulations of the authors' institutions and Food and Drug Administration guidelines, including patient consent where appropriate. For more information, visit the *JACC: Basic to Translational Science* author instructions page.

Manuscript received November 15, 2019; revised manuscript received August 26, 2020, accepted August 26, 2020.

of the BMPR2 predispose to PAH (3), but the exact and complete molecular landscape of factors interfacing with BMPR2-specific pathogenesis in PAH has not been fully defined. As compared to PAH, groups 2 and 3 PH (i.e., PH due to left heart disease and hypoxic lung disease) are considerably more prevalent; yet current targeted vasodilator therapies are mainly reserved for PAH. Furthermore, group 2 PH is often accompanied by an elevated PVR characteristic of PAH (1); under these circumstances, it can be difficult to distinguish between the 2 classifications without invasive hemodynamic study, and it is unknown whether this subgroup shares a common or distinct pathogenesis with PAH. Additional molecular insight would aid in the classification and management of these morbid yet heterogeneous subtypes of PH.

Despite progress in the era of pulmonary vasodilators, the 5-year mortality in PAH approaches 35% to 40% for incident and prevalent cases (4). The diagnosis of PAH remains challenging given its nonspecific clinical symptomatology and the necessity for invasive hemodynamics. Specifically, common acute or chronic pulmonary and cardiovascular diseases independent of PH often present with similar clinical features as PH such as dyspnea or exercise intolerance. Thus, PH can be overlooked, delaying diagnosis on average by 3 to 4 years and often until severe symptoms and RV failure present (5). Clinically, no reliable blood test is available to distinguish suspected PAH from other cardiopulmonary conditions and thus help to convince a clinician to pursue further invasive hemodynamic measurement. A recent study linking bone morphogenetic protein 9 (BMP9) plasma levels to portopulmonary hypertension (6), a subtype of WSPH group 1 PAH, indicated the diagnostic utility of utilizing BMP-specific ligands and partners of BMPR2 in this disease. Yet, to date, effective blood or plasma clinical biomarkers that correlate well with early pulmonary vasculature remodeling in PAH or with disease severity have been elusive (7).

Multiple subtypes of PH including PAH are driven by pulmonary endothelial cell (EC) dysfunction. It is thought that deficiency of BMPR2, either from genetic or acquired means, drives alterations of downstream signaling, leading to endothelial apoptosis and deficient angiogenesis and thus promoting vascular remodeling (3,8,9). Although the exact molecular mechanisms remain unclear, technologies are advancing that now allow for more direct investigation of BMPR2 deficiency directly in patients with predisposing mutations. Gu et al. (10) recently studied endothelial cells differentiated from human inducible pluripotent stem cells (iPSC-ECs) derived from 3 wild-type control subjects and 8 BMPR2-mutation positive carriers across 3 hereditary PAH families. Transcriptomic sequencing across these cells previously yielded insights about certain BIRC3-specific signaling pathways, but a comprehensive validation of all BMPR2-relevant factors differentially modulated with these mutations was not performed. We hypothesized that this dataset could offer an opportunity to identify additional crucial effectors and pathways in PAH pathogenesis.

In the present study, we reanalyzed the publicly available ribonucleic acid (RNA) sequencing dataset from Gu et al. (10) and found that the transcript for SCUBE1 was differentially expressed in iPSC-ECs carrying BMPR2 mutations. The protein structure of SCUBE1 carries both BMP1 and EGF domains and has been proposed as a direct BMP coreceptor (11). Increased circulating plasma SCUBE1 levels have been related to thromboembolic events, such as ischemic or hemorrhagic stroke, acute coronary syndrome, pulmonary embolism, and deep vein thrombosis (12–14), but the role of SCUBE1 in PAH has not been described. Guided by such sequencing, SCUBE1 was identified as a secreted factor down-regulated by multiple triggers of PAH and integral in BMPR2-specific endothelial pathophenotypes. Decreased SCUBE1 was found to be specific in the patient with PAH and correlated with the clinical features of pulmonary remodeling. These findings identified plasma SCUBE1 as a potential diagnostic tool and clinical biomarker that reflects the severity and progression of PAH and is inherently linked to disease pathogenesis and genetic predisposition.

METHODS

RNA-SEQUENCING ANALYSIS. The RNA-sequencing dataset from iPSC-ECs with and without BMPR2 mutations (10) was available at the National Center for Biotechnology Information Gene Expression Omnibus (GSE79613). Transcript abundances were quantified using Salmon (version 0.9, COMputational BIology and Network Evolution [COMBINE lab], University of Maryland, College Park, Maryland) (15), and the tximport (Bioconductor, international open source developer group [16]) (17) was used to assemble estimated count and offset matrices. The R package DESeq2 (version 1.20.0; R Foundation, Vienna, Austria) (18) was used to identify differentially expressed genes with adjusted p value of <0.05 by Benjamini-Hochberg method, and $|\log_2(\text{fold change})| > 1.5$.

RT-qPCR AND IMMUNOBLOTTING. RNA extraction and reverse transcription, quantitative polymerase chain reaction (RT-qPCR) were performed as we previously described (19). Quantitative PCR was

performed on an Applied Biosystems (Foster City, California) QuantStudio 6 Flex Fast Real-Time PCR device. Fold-change of RNA species was calculated using the formula $2^{-\Delta\Delta Ct}$, normalized to β-actin expression. SYBR qPCR primers for human SCUBE1 and β-actin were purchased from Bio-Rad Laboratories (Hercules, California). Taqman qPCR primers for human *BMPR2, HIFA, ANG, VEGF, NOS3, ANGPT1, LDHA, CPT1, PDK1, PECAM1, VWF,* and *β-actin* were purchased from Thermo Fisher Scientific (Waltham, Massachusetts).

For immunoblotting, cellular proteins were isolated using radioimmunoprecipitation assay lysis buffer and separated by sodium dodecyl sulfate-polyacrylamide gel electrophoresis and transferred to polyvinylidene fluoride membranes (Bio-Rad). Membranes were blocked in 5% nonfat milk or bovine serum albumin in tris-buffered saline buffer containing 0.1% Tween and incubated in the presence of the primary antibodies at 4°C overnight and then secondary antibodies for 1 h at room temperature. After washing in tris-buffered saline buffer containing 0.1% Tween, immunoreactive bands were visualized with the ECL system (Amersham Biosciences, Amersham, United Kingdom). The density of the bands was quantified by densitometric analysis using the ImageJ software (National Institutes of Health, Bethesda, Maryland).

Primary antibodies for SCUBE1 (ab105358, 1:500) and HIFA (1:500) were obtained from Abcam (Cambridge, United Kingdom); phospho-SMAD1/5/9 (13820S, 1:1,000), phospho-SMAD2/3 (8828S, 1:1,000), SMAD1 (9743S, 1:1,000), SMAD2/3 (3102S, 1:1,000) and β-Tubulin (2146, 1:5,000) were obtained from Cell Signaling Technology (Danvers, Massachusetts); and β-actin (sc-47778; 1:5,000) was obtained from Santa Cruz Biotechnology (Dallas, Texas). Appropriate secondary antibodies (anti-rabbit and anti-mouse) coupled to horseradish peroxidase were used (Dako Products, Agilent, Santa Clara, California).

CELL CULTURE AND REAGENTS. Primary human pulmonary arterial endothelial cells (PAECs) and human pulmonary arterial smooth muscle cells were grown in basal endothelial growth medium-2 and smooth muscle cell growth medium-2 supplemented with BulletKit (Lonza, Basel, Switzerland), respectively. All cells were cultured at 37°C in 95% air and 5% CO_2. Experiments were performed at passages 5 to 10. Recombinant human interleukin (IL)-1β was purchased from PeproTech (Rocky Hill, New Jersey) and used at concentrations of 10 ng/ml.

ELISA MEASUREMENT FOR CELL CULTURE MEDIUM, PLASMA, SERUM, AND TISSUE SCUBE1. Cell culture medium was collected at serial time points. Plasma or serum was derived from patient, mouse, or rat whole blood. The lung or myocardium tissue from human donor autopsy or from euthanized animals was homogenized with radioimmunoprecipitation assay buffer with proteinase inhibitor. The medium, plasma, serum, and tissue homogenate specimens were aliquoted and stored at −80°C. SCUBE1 levels were measured with human SCUBE1, rat Scube1, and mouse Scube1 enzyme-linked immunosorbent assay (ELISA) kits (OKEH01867, OKEI00879, and OKEH05018, respectively) purchased from Aviva Systems Biology (San Diego, California), according to the manufacturer's instructions.

SCUBE1 AND BMPR2 KNOCKDOWN AND LENTIVIRAL TRANSDUCTION OF SCUBE1 TRANSGENE. PAECs were transfected with SCUBE1 and BMPR2 small, interfering ribonucleic acid (siRNA) and Lipofectamine 2000 (Thermo Fisher Scientific). Nontargeted scrambled siRNA was used as control substance. The knockdown of target genes was confirmed with RT-qPCR.

Human SCUBE1 clone (SCUBE1-Bio-His, plasmid# 53415) was purchased from Addgene (Watertown, Massachusetts). A 2.9 kb SCUBE1-containing segment was cut and subcloned in pCDH-CMV-MCS-EF1-copGFP (System Biosciences, Mountain View, California) using NotI/AscI restriction enzymes (New England BioLabs, Ipswich, Massachusetts). The cloned plasmid was confirmed by deoxyribonucleic acid sequencing. HEK293T cells were cotransfected using Lipofectamine 2000 (Thermo Fisher Scientific) with lentiviral plasmids along with a packaging plasmid system (pPACK, System Biosciences), according to the manufacturer's instructions. Viral particles were harvested 48 h after transfection, concentrated, sterile filtered (0.45 μm), and lentiviral titers were determined. Human PAECs were then infected at 60% to 70% confluence (16 to 24 h incubation) with polybrene (8 ng/ml) for 2 to 3 days for gene transduction. The lentiviral parent vector expressing green fluorescent protein (GFP) was used as a control. The infection efficiency was assessed in each experiment by observing the GFP expression under a fluorescence microscope.

CELL EXPOSURE TO HYPOXIA. Primary cells were exposed for 48 h either to standard nonhypoxic cell-culture conditions (20% O_2, 5% CO_2, with N_2 balance at 37°C) or to hypoxia (0.2% O_2, 5% CO_2, with N_2 balance at 37°C) in a modular hypoxia chamber as previously described. Conditions were based on prior studies of human PAECs to allow for steady-state adaptation without nonspecific cell death.

BrdU PROLIFERATION AND CASPASE 3/7 APOPTOSIS ASSAYS. All bromodeoxyuridine (BrdU) proliferation and caspase 3/7 apoptosis assays were performed as we previously described and per the manufacturers' instructions: BrdU Cell Proliferation Assay Kit (#6813, Cell Signaling); Caspase-Glo 3/7 Assay (Promega, Madison, Wisconsin). For the caspase 3/7 assay, PAECs (10,000 cells/well) were incubated with Caspase-Glo 3/7 reagent in 96-well plate at room temperature for 1 h, then luminescence was recorded and normalized to protein content, as measured by bicinchoninic acid assay.

MATRIGEL TUBE FORMATION ASSAY. Capillary tube formation was performed using a commercial kit (Cultrex In Vitro Angiogenesis Assay Kit, #3470-096-K, R and D Systems, Minneapolis, Minnesota). Briefly, Matrigel (Corning Life Sciences, Corning, New York) with reduced growth factors was pipetted into pre-chilled 96-well plate (50 μl Matrigel per well) and polymerized for 30 min at 37°C. Following treatments, human PAECs (2×10^4 cells per well) were stained with Calcein AM (Cultrex, 1 μmol/l) for 30 min at 37°C, resuspended in 100 μl of basic media, and seeded in Matrigel-coated 96-well plate. After 4 to 6 h of incubation, tubular structures were photographed using an Olympus inverted microscope (Olympus Corporation, Tokyo, Japan) with a 20× magnification. The number of branch joint points was quantified by a blinded observer in triplicate determinations from 3 separate experiments.

PAH ANIMAL MODELS. PAH rat models. As we previously described (19), male Sprague-Dawley rats (10 to 14 weeks old; Charles River Laboratories, Wilmington, Massachusetts) were injected with 60 mg/kg monocrotaline, or injected with 20 mg/kg SU5416 (Sigma Aldrich, St. Louis, Missouri) followed by 3 weeks of normobaric hypoxia (10% O_2) and 2 weeks of normoxia. Prior to euthanasia, right heart catheterization (RHC) was performed to confirm elevated PAP. Thereafter, plasma and lung tissues were collected and stored at −80°C for further studies.

PAH mouse model. As we recently reported (19), pulmonary inflammation resulting in severe PH in mouse was elicited in pulmonary IL-6 transgenic mice treated with hypoxia. C57BL/6 IL-6 transgenic male mice (10 to 12 weeks old) were subjected to 21 days of normobaric hypoxia (10% O_2). Right heart catheterization was performed post-exposure, followed by tissue harvest. These rat and mouse procedures were approved by the Institutional Animal Care and Use Committee at the University of Pittsburgh (protocol number 16129515).

EXPERIMENTAL BACTERIAL PNEUMONIA MOUSE MODEL. A *Klebsiella pneumoniae* bacterial pneumonia mouse model was generated as previously described (20). Briefly, C57Bl/6J mice (JAX #000664, Jackson Laboratory, Bar Harbor, Maine) were anesthetized and 100 μl of *K. pneumoniae* bacterial slurry (strain 43816, serotype 2, American Type Culture Collection, Manassas, Virginia) was administered intratracheally. Age- and sex-matched mice were used for experiments. Forty-eight hours after *K. pneumoniae* inoculation, mice were euthanized, and blood and lung tissue were collected. All procedures were performed with approval of the Institutional Animal Care and Use Committee at the University of Pittsburgh (protocol number 18063096).

ACUTE MYOCARDIAL INFARCTION MOUSE MODEL. Acute myocardial infarction in C57Bl/6J mice was induced by ligating the left coronary artery as previously described (21). Briefly, mice were anesthetized and intubated. Thoracotomy was performed and the pericardium was opened followed by permanent ligation of the left coronary artery at the site of the vessel's emergence past the tip of the left atrium. Myocardium histology was performed to delineate myocardial infarction. Sham-operated mice underwent the same procedure without coronary artery ligation. The plasma and left ventricular myocardium were collected on day 5 after surgery. All procedures were approved by the Institutional Animal Care and Use Committee at the University of Pittsburgh (protocol number 18083562).

HUMAN SUBJECTS. For all the human subjects enrolled in study, informed consent was universally obtained, and all study procedures conformed to the ethical standards of the Declaration of Helsinki. All patients with known or suspected PH and referred for RHC during their routine clinical care from 2014 to 2018 at 2 designated PH Comprehensive Care Centers—the University of Pittsburgh Medical Center (UPMC) and the Hospital of the University of Pennsylvania (HUP)—were eligible for inclusion. A total of 66 PH patients were from UPMC, including 52 group 1 PAH patients and 14 group 2 PH patients; 12 PH patients were from HUP, including 10 group 1 PAH patients and 2 group 2 PH patients. Procedures indicated for either diagnostic or disease-monitoring purposes were included. Patients were prospectively enrolled by study staff before RHCs were performed. The study protocol was approved separately by the institutional review boards (IRBs) from each respective institution (IRB no. STUDY19050364, University of Pittsburgh; IRB no. 818660, University of Pennsylvania). Non-PH control blood samples were

collected from patients with RHC data confirming no PH (22 from UPMC and 9 from HUP), combined with 25 subjects from an established control cohort with no known pulmonary or cardiovascular diseases (IRB no. STUDY19070274).

Subjects with chronic obstructive pulmonary disease (COPD) were randomly selected from the Emphysema Research Registry in the University of Pittsburgh, each carrying a forced expiratory volume to forced vital capacity ratio of <0.7 and predicted forced expiratory volume <80% but predicted CO diffusing capacity >55%. The study was approved by the Institutional Review Board for Human Subject Research at the University of Pittsburgh (IRB no. STUDY19120059).

Mechanically ventilated patients in the medical or cardiac intensive care units at UPMC were enrolled in the University of Pittsburgh Acute Lung Injury and Biospecimen Repository from October 2011 to February 2020. For the present study, a subset of subjects (n = 39) was selected from the cohort, meeting diagnostic criteria for the acute respiratory distress syndrome according to the Berlin criteria (22). Blood samples within 48 h of intubation were collected from enrolled subjects. The study was approved by the University of Pittsburgh Institutional Review Board (IRB no. STUDY19050099).

Coronary artery disease (CAD) patients and age-, sex-, and race-matched non-CAD control subjects were selected from an ongoing PCI (Percutaneous Coronary Intervention) Registry at UPMC. CAD was defined by coronary angiogram showing ≥50% stenosis requiring percutaneous coronary intervention. Control patients were defined with 0% to 49% stenosis on coronary angiography. The study was approved by the University of Pittsburgh IRB (IRB no. STUDY990835).

RIGHT HEART CATHETERIZATION. Clinically indicated RHCs were performed following a standard clinical protocol. A pulmonary artery (PA) catheter (Edwards, Irvine, California) was advanced into the central venous system (superior vena cava), right atrium, RV, and PA by experienced operators in individuals at rest in the supine position after appropriate catheter calibration and zeroing. Pressure waveforms from the right atrium, PA, and pulmonary capillary wedge positions were recorded in duplicate at end-expiration using the Xper Cardio Physiomonitoring System at UPMC (Philips, Melbourne, Florida) and Horizon Cardiology Cardiovascular Information System at HUP (McKesson, San Francisco, California). Cardiac output was calculated by the Fick method using main PA and peripheral oxyhemoglobin saturations. PVR was calculated based on the transpulmonary pressure gradient (mean PAP- pulmonary capillary wedge pressure [PCWP]) divided by cardiac output.

Screening for WSPH group 1 PAH was first performed by evaluation of hemodynamics, namely via a mean pulmonary arterial pressure (mPAP) >20 mm Hg, a PCWP <15 mm Hg, and a PVR > 3 Wood units. These hemodynamic criteria followed the recently updated 2019 classification criteria (1); notably, these samples predominantly fit the 2013 classification scheme as well (23), because a vast majority of patient recruitment for blood samples was performed prior to 2018. After hemodynamic identification, third-party expert clinicians reviewed clinical notes and relevant studies for a determination of WSPH Pulmonary Hypertension Classification. Notably, a group 1 PAH diagnosis was made only after excluding patients with confounding variables from etiologies more consistent with left heart disease, hypoxic lung disease, and chronic thromboembolism. Group 2 PH was defined by elevated mPAP with PCWP ≥15 mm Hg and known left heart disease, again as reviewed by third-party expert clinicians.

TRANSTHORACIC ECHOCARDIOGRAPHY. Transthoracic echocardiographic images of 49 PAH patients from UPMC were analyzed by a third-party clinician not involved directly in each patient's clinical care. Only transthoracic echocardiographic studies performed within 3 months of the date of RHC and blood sample collection were analyzed. The measurement of RV dimensions, tricuspid annular plane systolic excursion, and criteria for RV hypertrophy and dilation were based on standard protocol and American Society of Echocardiography consensus (24).

BLOOD SAMPLE, LUNG, AND HEART TISSUE COLLECTION. Peripheral blood samples were drawn from human subjects as we have already described. Samples were transferred into BD Vacutainer tubes (Becton, Dickinson, and Company, Franklin Lakes, New Jersey), followed by standard plasma or serum separation.

Lung tissues from nondiseased normal control subjects and PAH and COPD patients, as well as myocardial tissues from nondiseased control subjects, ischemic cardiomyopathy (ICM), and nonischemic cardiomyopathy (NICM) patients were collected from rapid lung biopsy or lung/heart transplant procedures, flash frozen, and stored at −80°C at UPMC. These procedures were approved by the IRB at UPMC (IRB no. PRO14010265 and Committee for Oversight of Research Involving the Dead no. 722).

STATISTICAL ANALYSIS. All data are represented as mean ± SD or median with interquartile range (IQR),

depending on data distribution. For cell culture data, these represent at least 3 independent experiments performed in triplicate. Normality of data distribution was confirmed by Shapiro-Wilk testing. The categorical variables are presented as counts and percentages. For comparisons between 2 groups, a 2-tailed Student's *t*-test was used for normally distributed data. For comparisons among more than 2 normally distributed groups, 1-way analysis of variance testing was performed with post hoc Bonferroni test. For non-normally distributed data, Mann-Whitney *U* test was performed for pairwise comparisons; Kruskal-Wallis test was performed with post hoc Dunn Multiple Comparison test for comparisons among non-normally distributed groups. A p value if <0.05 was considered significant. Nonparametric Spearman rank correlation was performed to determine the association of variables with calculated correlation coefficient (*rho*). Receiver-operating characteristic (ROC) analysis was performed using the statistics package included with GraphPad Prism software (version 8.30, GraphPad Inc., San Diego, California). The area under the curve (AUC) (C-statistics) was calculated using trapezoidal rule for empirical sensitivity and 1-specificity in any cutpoint (25). The test sensitivity and specificity at various thresholds were calculated by the Clopper-Pearson method (26). The optimal cutpoint in ROC curve was determined by Youden test (27). A diagnostic odds ratio (OR) for the optimal cutpoint was calculated by dividing the positive likelihood ratio over the negative likelihood ratio, as previously reported (28).

RESULTS

RNA-SEQUENCING DATA FROM BMPR2-MUTANT iPSC-ECs IDENTIFY SCUBE1 AS A FACTOR INTEGRALLY LINKED TO PAH PATHOGENESIS. Publicly available RNA-sequencing data of human iPSC-ECs derived from 3 wild-type control subjects and 8 BMPR2-mutation positive carriers across 3 hereditary PAH families (10) were analyzed via Salmon (15) and DESeq2 with the intent to define differentially expressed genes in BMPR2-mutant cells after adjustment for false discovery rate. As shown in **Table 1**, 17 transcripts were identified as being significantly differentially expressed between BMPR2-mutant and wild-type control subjects ($|\log_2(\text{fold change})| > 1.5$ and adjusted $p < 0.05$). Of these transcripts, a systematic publications search revealed functional relevance to BMP signaling for 2 genes (*SCUBE1* and *MX1*) (29,30) and relevance to the related transforming growth factor (TGF) superfamily pathway for 1 gene, *CDH6* (31). In contrast to the more indirect downstream signaling connections reported for *MX1* and *CDH6*, *SCUBE1*, which encodes SCUBE1, carries a unique molecular structure including both BMP1 and EGF domains and has been proposed as a direct BMP coreceptor (11). Such direct links to BMPR2 made SCUBE1 a promising candidate for further analysis in endothelial function and PAH pathogenesis.

GENETIC AND ACQUIRED PAH TRIGGERS MODULATE SCUBE1 EXPRESSION IN CULTURED PAECs. As shown in **Figure 1A**, immunoblotting demonstrated substantial expression of SCUBE1 in PAECs but not in PA smooth muscle cells, suggesting endothelial-specific enrichment in the pulmonary vasculature. In cultured PAECs, the effects on SCUBE1 expression of various genetic and acquired triggers of PAH were examined. Chronic exposure to inhibitory RNA (siRNA) knockdown of BMPR2 in PAECs significantly down-regulated SCUBE1 at transcript, secreted, and intracellular protein levels (**Figures 1B, 1C, and 1F**; and see Supplemental Figure S1A, showing the efficacy of siRNA knockdown on BMPR2 transcript). The down-regulation in SCUBE1 across transcript, secreted protein, and intracellular protein levels was also observed in PAECs treated with hypoxia or the inflammatory cytokine IL-1β, 2 well-known acquired triggers for PAH (**Figures 1D to 1F**).

To rule out that down-regulation of SCUBE1 by specific PAH triggers is secondary to a general suppression of PAEC activity and viability, we quantified the levels of known regulators of endothelial function in PAECs exposed to hypoxia and IL-1β. The expression of angiogenesis-, proliferation-, and apoptosis-related genes *ANG, VEGF, NOS3,* and *ANGPT1*; adhesion molecule genes *PECAM1* and *VWF;* and endothelial metabolism-associated genes *PDK1, LDHA,* and *CPT1* were profiled. As shown in Supplemental Figure S2, most endothelial genes examined were up-regulated by hypoxia (*VEGF*, *NOS3, ANG, ANGPT1, VWF, PDK,* and *LDHA),* with a down-regulation of *CPT1* only and no significant change to *PECAM1.* When PAECs were treated with IL-1β, the expression of *VEGF, NOS3,* and *PECAM1* was increased, whereas the expression of other genes was decreased (*ANGPT1, VWF,* and *CPT1*) or remained unchanged (*ANG, PDK1,* and *LDHA).* In total, these findings demonstrated an expected and specific set of reprogramming events in viable endothelium in response to hypoxia and inflammatory stress. In this context, these results suggested that specific down-regulation of SCUBE1 may coordinate with other stress-responsive signaling pathways to control endothelial function in the setting of PAH.

TABLE 1 Genes Differentially Expressed in RNA-Sequencing Data From iPSC-ECs Derived From Affected BMPR2 Mutant Patients and Wild-Type Control Subjects

Gene	Adjusted p Value	Functional Relevance
IFI44L	<0.001	Interferon response
C1QTNF3	<0.001	PKC signaling
CDH6	0.001	TGF signaling (31)
SCUBE1	0.001	BMP/TGF signaling (30,50)
RARB	0.003	DNA demethylation
CALN1	0.004	Calcium-binding protein
DBF4P1	0.004	Pseudogene
NRG3	0.006	EGF-like signaling
MX1	0.006	BMP signaling (29) Interferon response
BST2	0.02	Interferon response
H19	0.02	Noncoding RNA
IFI6	0.02	Interferon response
IFIT1	0.02	Interferon response
CRHBP	0.02	Chromosome segregation
FAM65B	0.03	RhoA-related migration
TMEM200C	0.03	Unknown function
ST8SIA6	0.04	PI3K/Akt signaling

BMP = bone morphogenetic protein; DNA = deoxyribonucleic acid; EGF = epidermal growth factor; iPSC-EC = induced pluripotent stem cell-endothelial cell; PI3k = phosphoinositide 3-kinase; PKC = protein kinase C; RNA = ribonucleic acid; TGF = transforming growth factor.

HIF1A MEDIATES SCUBE1 DOWN-REGULATION BY HYPOXIA AND IL-1β BUT NOT BMPR2 KNOCKDOWN. HIF1A is a master regulatory factor that controls hypoxic reprogramming in endothelial cells. In addition to true hypoxia, inflammatory cytokines such as IL-1β also induce HIF1A accumulation (32). To determine the involvement of HIF1A in SCUBE1 down-regulation by these acquired PAH triggers, HIF1A siRNA knockdown was performed. The efficacy of siRNA knockdown of the *HIF1A* gene in PAECs was confirmed by RT-qPCR (Supplemental Figure S1B). As shown in **Figure 2A**, intracellular HIF1A levels were increased in PAECs exposed to hypoxia or IL-1β but remained unchanged with BMPR2 siRNA knockdown. Correspondingly, whereas hypoxia and IL-1β consistently decreased SCUBE1 transcript levels in PAECs treated with nonspecific scrambled control RNA, HIF1A knockdown nearly completely reversed SCUBE1 down-regulation induced by hypoxia and IL-1β (**Figures 2B and 2C**), which appeared to be independent of BMPR2 expression as evidenced by the unchanged *BMPR2* expression profile with HIF1A knockdown (**Figure 2D**). Conversely, consistent with the lack of dependence of HIF1A expression on BMPR2, HIF1A knockdown did not alter the extent of SCUBE1 down-regulation driven by BMPR2 deficiency (**Figure 2C**).

SCUBE1 REGULATES ANGIOGENIC POTENTIAL, PROLIFERATION, AND APOPTOSIS IN CULTURED PAECs. To determine the function of SCUBE1 in the control of PAEC activity, we conducted loss- and gain-of-function analyses with manipulation of SCUBE1 expression in PAECs by siRNA knockdown (**Figures 3A and 3B**) and forced SCUBE1 expression with lentiviral transduction of a SCUBE1 transgene, respectively (**Figures 3F to 3H**). SCUBE1 knockdown in PAECs significantly inhibited tube formation of PAECs in Matrigel (**Figure 3C**), inhibited PAEC proliferation as determined by BrdU incorporation (**Figure 3D**), and increased apoptosis as indicated by caspase 3/7 activity (**Figure 3E**). Conversely, forced SCUBE1 overexpression in PAECs enhanced tube formation (**Figure 3I**), increased proliferation (**Figure 3J**), and decreased apoptosis (**Figure 3K**). Taken together, these results demonstrate that SCUBE1 is both necessary and sufficient to invoke a protective function against PAH in the pulmonary endothelium, controlling a proangiogenic effect and augmenting survival and proliferative capacity.

SCUBE1 CONTROLS THE ACTIVATION OF BMPR2-RELEVANT SMAD-SIGNALING MEDIATORS. Prior reports have suggested SCUBE1 may act as a binding partner and coactivator of BMPR2 receptor, via the BMP domain located at the N-terminus of the protein (11). To clarify this functionality of SCUBE1 in PAECs, BMPR2- and TGF-β-specific SMAD-signaling mediators were quantified under SCUBE1 knockdown or forced expression. As shown in **Figure 4A**, although SCUBE1 knockdown or overexpression significantly altered the intracellular SCUBE1 protein in PAECs, it did not change BMPR2 transcript level. In contrast, such knockdown and forced expression of SCUBE1 significantly reduced and increased levels, respectively, of activated and phosphorylated SMAD1/5/9 relevant to BMPR2 activation (**Figures 4B and 4C**). The manipulation of SCUBE1, either via siRNA knockdown or forced expression, had no influence on activated and phosphorylated SMAD2/3 relevant to TGF-β-relevant signaling (**Figures 4B and 4D**). These results support the notion that SCUBE1 functions primarily through BMPR2-relevant SMAD signaling in PAECs.

Scube1 LEVELS ARE DECREASED IN PLASMA AND LUNG TISSUE IN PAH RODENT MODELS. To determine the relevance of SCUBE1 regulation to PAH, secreted Scube1 levels in plasma and lung tissue homogenates were quantified by ELISA in 3 well-established PAH animal models: monocrotaline-exposed rats; SU5416-chronic hypoxia-exposed PAH rats; or pulmonary-specific IL-6 transgenic mice exposed to chronic hypoxia (19). As shown in

FIGURE 1 SCUBE1 Is Enriched in Pulmonary ECs and Down-Regulated by Triggering Factors Driving PAH

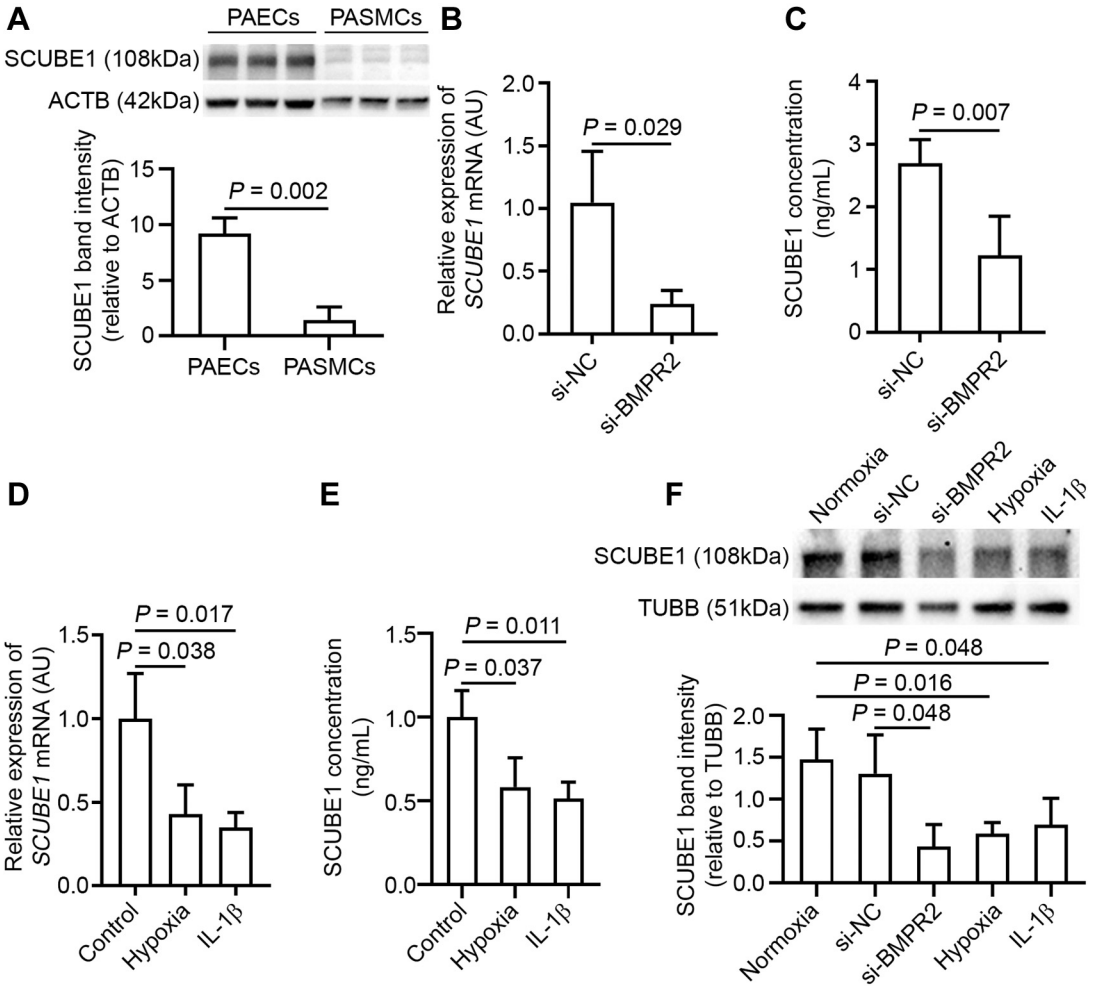

(A) Abundance of secreted SCUBE1 protein in conditioned media from human pulmonary arterial endothelial cells (PAECs) and pulmonary arterial smooth muscle cells (PASMCs) was determined by immunoblotting (n = 3 samples per group). **(B,C)** PAECs were treated with control small, interfering ribonucleic acid (si-NC) or small, interfering ribonucleic acid specific to BMPR2 (si-BMPR2) for 72 h after which **(B)** SCUBE1 messenger ribonucleic acid (mRNA) expression was measured by reverse transcription, quantitative polymerase chain reaction of cellular homogenates (n = 3 samples per group) and SCUBE1 protein abundance was quantified by **(C)** enzyme-linked immunosorbent assay of conditioned media (n = 4 samples per group). **(D,E)** Similarly, PAECs were stimulated with hypoxia or interleukin (IL)-1β for 48 h, after which SCUBE1 **(D)** mRNA (n = 3 samples per group) and **(E)** secreted protein (n = 3 samples per group), were quantified by reverse transcription, quantitative polymerase chain reaction and enzyme-linked immunosorbent assay, respectively. **(F)** Immunoblot of PAEC homogenates (n = 3 samples per group) after the above-mentioned treatments. Immunoblots are representative of 3 independent experiments with band intensities quantified by densitometry. Values are presented as mean ± SD. The p values were calculated by Student's *t*-test, 1-way analysis of variance with post hoc Bonferroni test. The comparisons with p > 0.05 were not explicitly stated in the panels. AU = arbitrary units; PAH = pulmonary arterial hypertension.

Figures 5A to 5F, in these 3 PAH rodent models, Scube1 levels were down-regulated significantly in both diseased plasma and lung tissues as compared with those in control animals.

To define the specificity of the Scube1 decrease compared with other rodent models of cardiopulmonary disease, plasma and tissue Scube1 levels were measured in mice with acute bacterial pneumonia induced by *K. pneumoniae* inoculation and acute myocardial infarction induced by left coronary artery ligation. As shown in Figures 5G to 5J, both plasma and organ tissue (lung or heart) Scube1 levels were significantly increased in the rodents with acute pneumonia or acute myocardial ischemia.

FIGURE 2 HIF1A Expression Is Induced by Both Hypoxia and Il-1β and Mediates SCUBE1 Down-Regulation

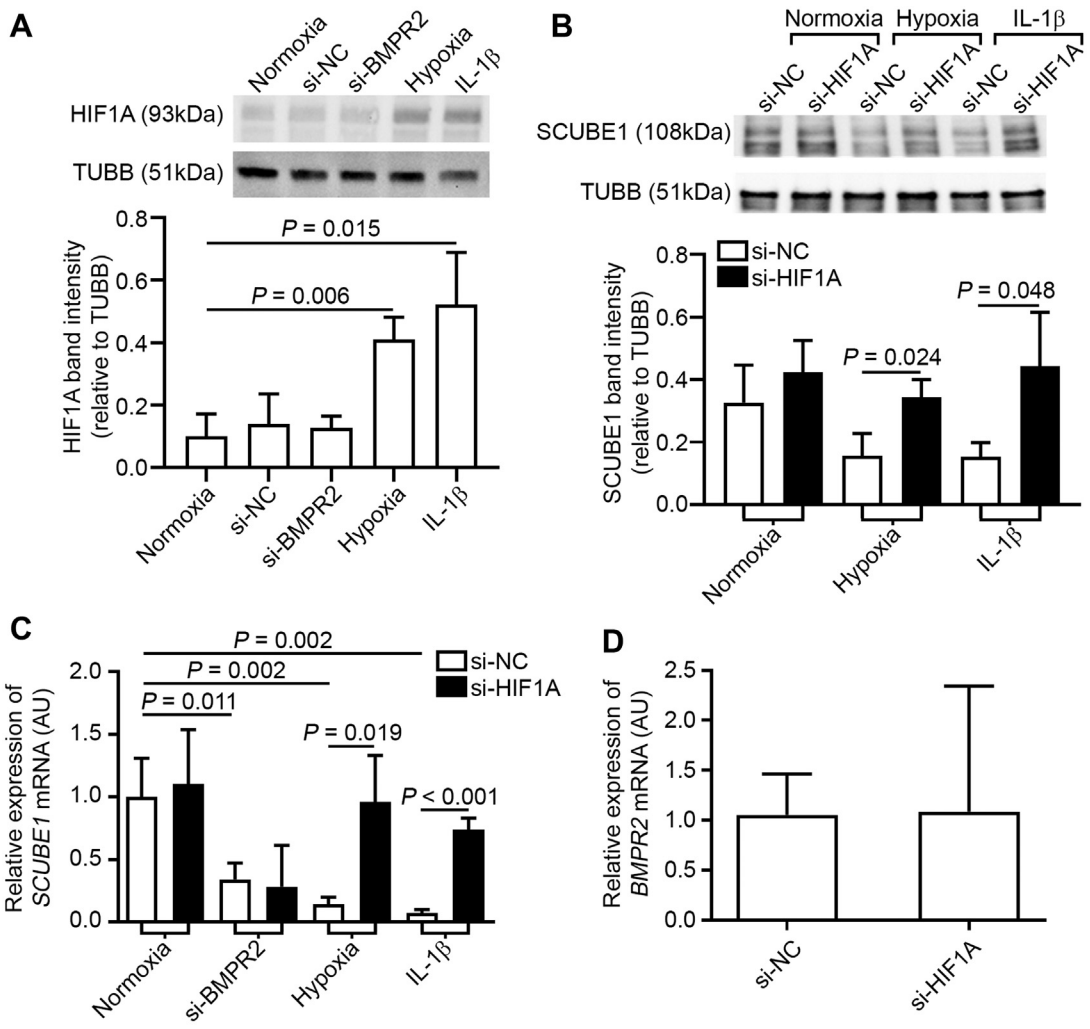

(A) PAECs were treated with si-NC, si-BMPR2, hypoxia, and IL-1β for 48 h, and HIF1A protein expression was determined by immunoblotting (n = 3 samples per group). **(B)** PAECs were treated with either si-NC or small, interfering ribonucleic acid to HIF1A and exposed to normoxia, hypoxia, or IL-1β, followed by immunoblotting for SCUBE1 (n = 3 samples per group). **(C)** In addition to the above-mentioned conditions, PAECs were also treated with si-BMPR2, and mRNA expression was determined by reverse transcription, quantitative polymerase chain reaction (n = 3 to 6 samples per group). **(D)** BMPR2 mRNA expression was quantified in PAECs treated with either si-NC or si-HIF1A (n = 3 samples per group). Immunoblots are representative of 3 independent experiments with band intensities quantified by densitometry. Values are presented as mean ± SD. The p values were calculated by Student's *t*-test, 1-way analysis of variance with post hoc Bonferroni test. The comparisons with p > 0.05 were not explicitly stated in the panels. Abbreviations as in Figure 1.

SCUBE1 LEVELS ARE DECREASED IN PLASMA AND LUNG TISSUE FROM PAH PATIENTS. Because SCUBE1 is a secreted factor inherently relevant to endothelial pathophenotypes in PAH and based on the above-mentioned rodent studies, we postulated that differential plasma levels in humans may be utilized to distinguish PAH from other cardiopulmonary diseases. Plasma specimens were collected from 62 patients with WSPH group 1 PAH and 16 patients with WSPH group 2 PH at 2 separate U.S. PH referral centers and were confirmed clinically and hemodynamically by invasive RHC. As comparisons, 56 non-PH individuals, 39 patients with COPD, and 39 patients with acute lung injury (ALI) or clinical acute respiratory distress syndrome were included for plasma SCUBE1 measurement. Supplemental Tables S1 to S3 describe the demographics and available hemodynamic profiles of these study patients at the time of

FIGURE 3 SCUBE1 Levels Modulate EC Pathophenotypes in Cultured PAECS

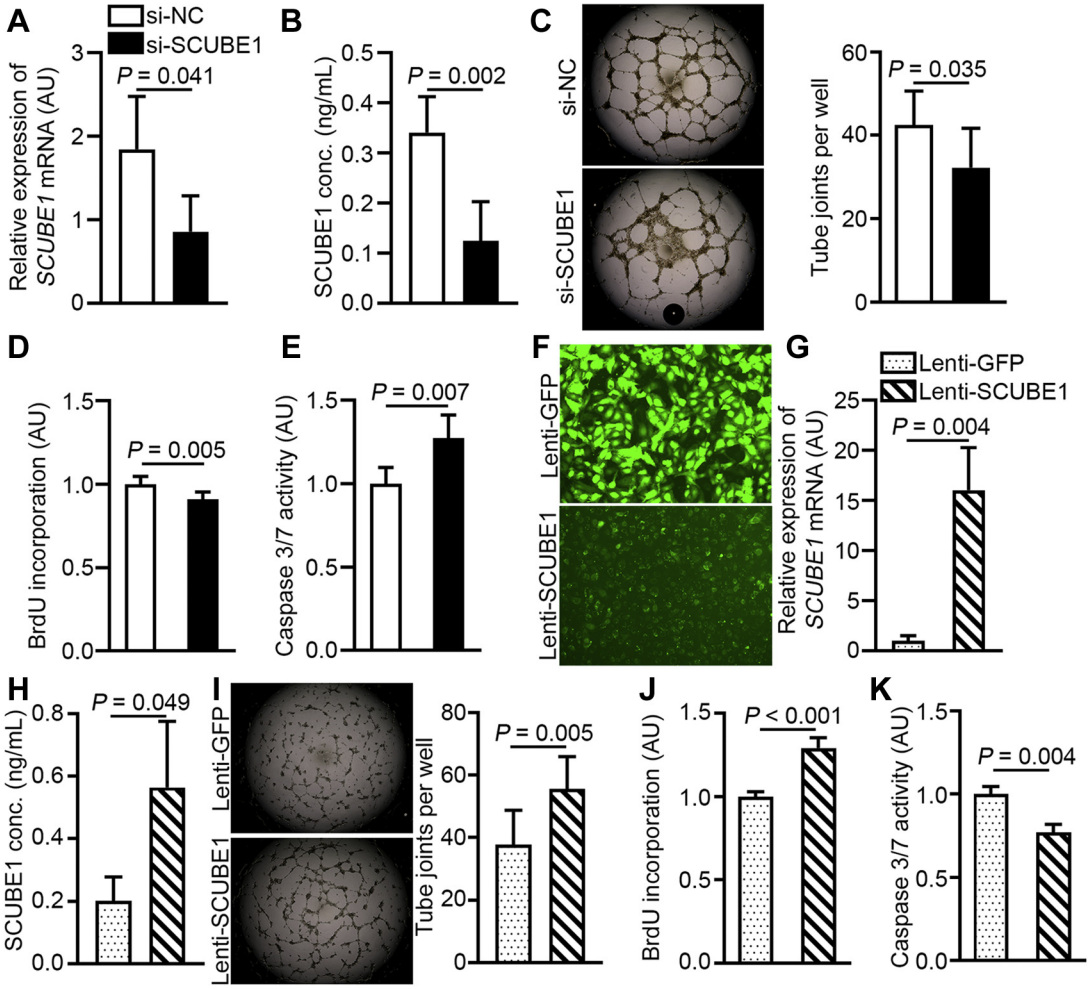

(A to E) PAECs were treated with si-NC or SCUBE1-specific small, interfering ribonucleic acid (si-SCUBE1). SCUBE1 mRNA levels were determined by reverse transcription, quantitative polymerase chain reaction (n = 4 samples per group) **(A)** and secreted SCUBE1 protein was quantified by enzyme-linked immunosorbent assay of conditioned media (n = 5 samples per group) **(B)**. **(C)** Angiogenic potential of cultured PAECs was determined by tube formation assay and quantification of joint counts in Matrigel (n = 8 samples per group). PAEC proliferation and apoptosis were determined by bromodeoxyuridine (BrdU) incorporation normalized to cell counts (n = 6 to 7 samples per group) **(D)** and caspase 3/7 activity normalized to total protein concentration (conc) (n = 5 sample per group) **(E)**, respectively. **(F–K)** SCUBE1 overexpression in PAECs was achieved through lentiviral vector (Lenti) transduction expressing a green fluorescent protein (GFP) reporter without (Lenti-GFP) or with a SCUBE1 transgene (Lenti-SCUBE1). To determine transgene delivery efficiency, fluorescent microscopy images of GFP protein expression were obtained **(F)**, mRNA quantification by reverse transcription, quantitative polymerase chain reaction was performed (n = 3 samples per group) **(G)**, and secreted protein accumulation was confirmed by enzyme-linked immunosorbent assay (n = 3 samples per group) **(H)**. **(I to K)** Alterations of angiogenic potential, proliferation, and apoptosis by Lenti-SCUBE1 were determined by joint counts in Matrigel tube formation assays (n = 8 samples per group) **(I)**, BrdU incorporation normalized to cell count (n = 4 samples per group) **(J)**, and caspase 3/7 activity normalized to total protein concentration (n = 3 samples per group) **(K)**, respectively. Matrigel images are representative of 8 independent samples. Values are presented as mean ± SD. The p values were calculated by Student's *t*-test. Abbreviations as in Figure 1.

blood draw. As shown in Figure 6A and quantified by ELISA, plasma SCUBE1 levels from patients with PAH (median: 2.70 ng/ml; IQR: 1.80, 4.76 ng/ml) were significantly lower than those from control subjects without PAH (median: 5.84 ng/ml; IQR: 3.51 to 9.10 ng/ml; $p < 0.001$), patients with COPD (median: 4.81 ng/ml; IQR: 3.23 to 6.78 ng/ml; $p = 0.007$), and patients with ALI (median: 8.61 ng/ml; IQR: 2.65 to 12.17 ng/ml; $p < 0.001$). Additionally, we collected lung tissues from rapid autopsy or transplant lungs derived from 8 patients with PAH, 11 control subjects without PAH, and 20 patients with COPD. Demographics of tissue

FIGURE 4 pSMAD1 Connects SCUBE1 Expression to BMPR2 Signaling

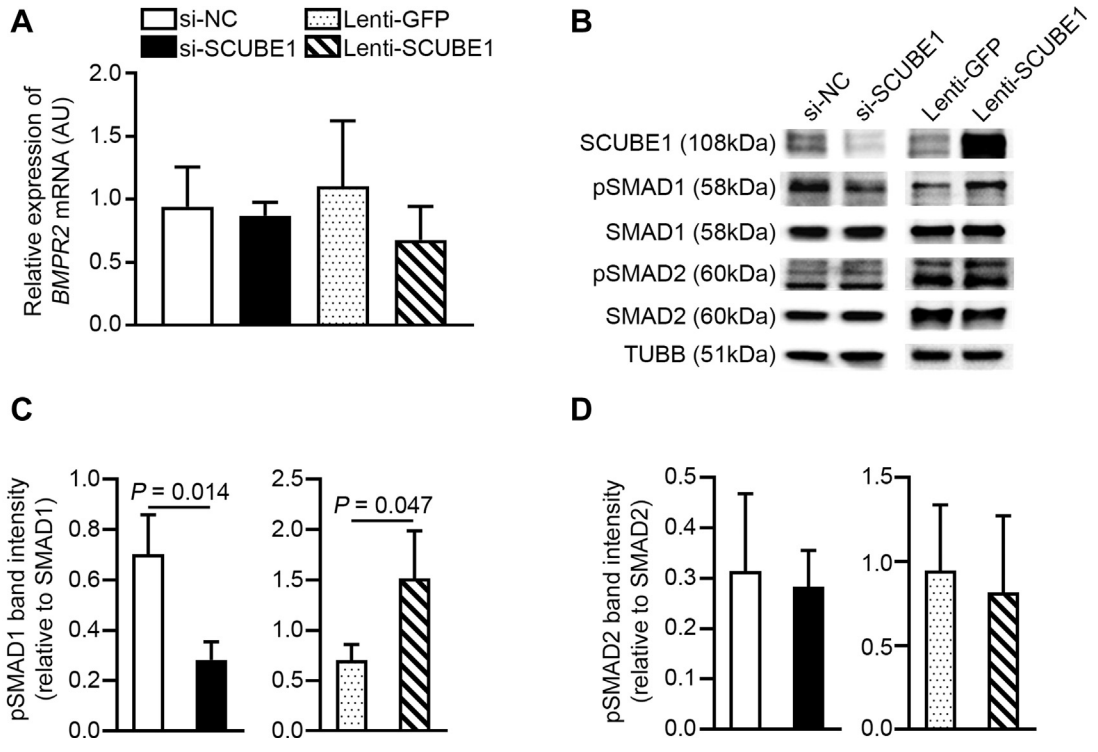

PAECs were treated with (si-NC, si-SCUBE1, Lenti-GFP, or Lenti-SCUBE1. **(A)** BMPR2 mRNA levels were determined by reverse transcription, quantitative polymerase chain reaction (n = 4 samples per group). **(B–D)** Immunoblotting was performed to quantify for phosphorylated fraction of Smad1/5/9 (pSMAD1) and of Smad2/3 (pSMAD2) as well as total SMAD1 and SMAD2 **(B)**. Ratios of phosphorylated to total SMAD1/5/9 (n = 3 samples per group) **(C)** and SMAD2/3 (n = 3 samples per group) **(D)** were determined by densitometric analysis. Immunoblots are representative of 3 independent experiments. Values are presented as mean ± SD. The p values were calculated by Student's *t*-test. The comparisons with $p > 0.05$ were not explicitly stated in the panels. Abbreviations as in Figures 1 and 2.

donors are listed in Supplemental Table S4. As shown in **Figure 6B**, correlating with decreased levels in PAH plasma, SCUBE1 levels in lung tissue from patients with PAH (median: 4.00 ng/mg tissue; IQR: 2.98, 5.08 ng/mg tissue) were significantly lower than those from control subjects without PAH (median: 6.93 ng/mg tissue; IQR: 4.38 to 8.28 ng/mg tissue; $p = 0.034$) and patients with COPD (median: 6.15 ng/mg tissue; IQR: 4.05 to 9.54 ng/mg tissue; $p = 0.049$).

In contrast to these findings in patients with PAH, plasma SCUBE1 levels in patients with WSPH group 2 PH (median: 5.02 ng/ml; IQR: 1.98 to 8.06 ng/ml) were, on average, significantly higher than those for PAH patients ($p = 0.026$) (**Figure 6C**). Patients' demographics and hemodynamics were listed in Supplemental Tables S1 and S2. Beyond lung disease, we sought to further clarify the specificity of decreased SCUBE1 expression in plasma, as SCUBE1 is known to change in the setting of ischemic heart disease (12). SCUBE1 levels were quantified in serum samples from 21 patients with CAD confirmed by coronary angiography versus 22 patients without obstructive CAD. In parallel, SCUBE1 was also measured from left ventricular myocardial samples isolated from 12 patients with NICM and 12 patients with ICM (see Supplemental Tables S5 and S6 for patient demographics). As shown in **Figures 6D and 6E**, SCUBE1 serum levels were significantly higher in patients with CAD and in heart tissues from patients with ICM, when comparing to those from control subjects without CAD.

To evaluate the diagnostic value of plasma SCUBE1 measurement in PAH, we performed an ROC analysis between PAH and a combined non-PAH cohort composed of control, COPD, and ALI subjects (**Figure 6F**), resulting in an AUC of 0.75 ($p < 0.001$). An optimal plasma SCUBE1 cutpoint of 5.46 ng/ml was defined to distinguish PAH from the non-PAH cohorts with a high specificity of 0.87 and a sensitivity of 0.53

FIGURE 5 **Scube1 Expression Is Decreased in Rodent Models of PAH**

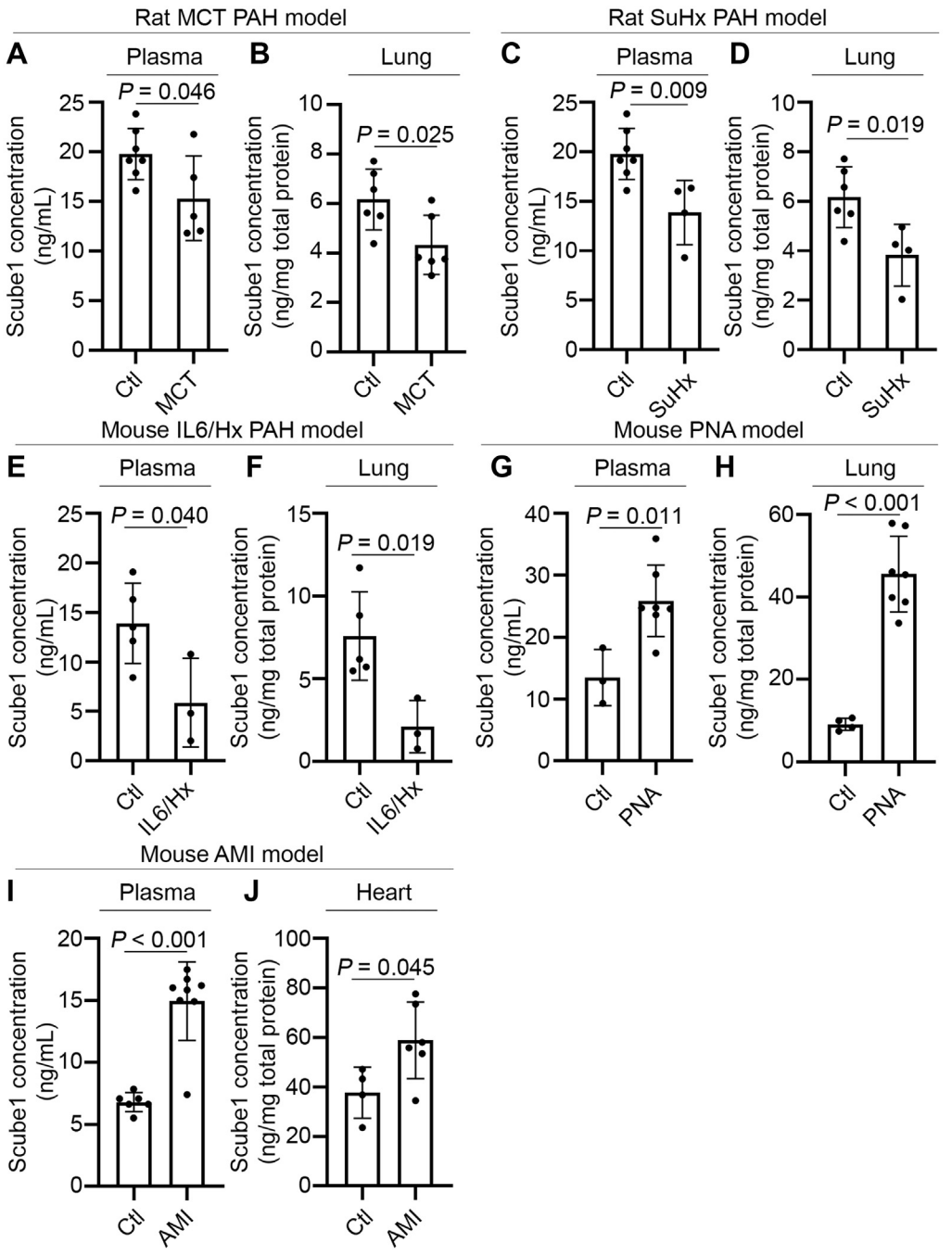

Male Sprague-Dawley rats were injected with monocrotaline (MCT) (versus vehicle control [Ctl]) or injected with SU5416 (SuHx) and exposed chronically to 10% O_2 for 3 weeks followed by 2 weeks of normoxia (vs. vehicle Ctl in normoxia). Male C57BL/6 interleukin (IL)-6 transgenic mice were subjected to 3 weeks of hypoxia (10% O_2) exposure (IL6/Hx) versus normoxia Ctl. Acute bacterial pneumonia (PNA) was generated in male and female C57/BL mice at 0 h (baseline Ctl) and after 48 h following intratracheal administration of *K. pneumoniae*. Acute myocardial infarction (AMI) was induced by direct ligation of left coronary artery (vs. sham surgery Ctl) for 5 days in C57BL/6 mice. Scube1 protein levels were determined by enzyme-linked immunosorbent assay in plasma (n = 3 to 7 per group) **(A,C,E,G,I)** and lung or heart tissue homogenate (n = 3 to 6 per group) **(B,D,F,H,J)** collected from euthanized animals. Values are presented as mean ± SD. The p values were calculated by Student's *t*-test. PAH = pulmonary arterial hypertension.

FIGURE 6 Plasma SCUBE1 Levels Are Decreased in Patients With WSPH Group 1 PAH

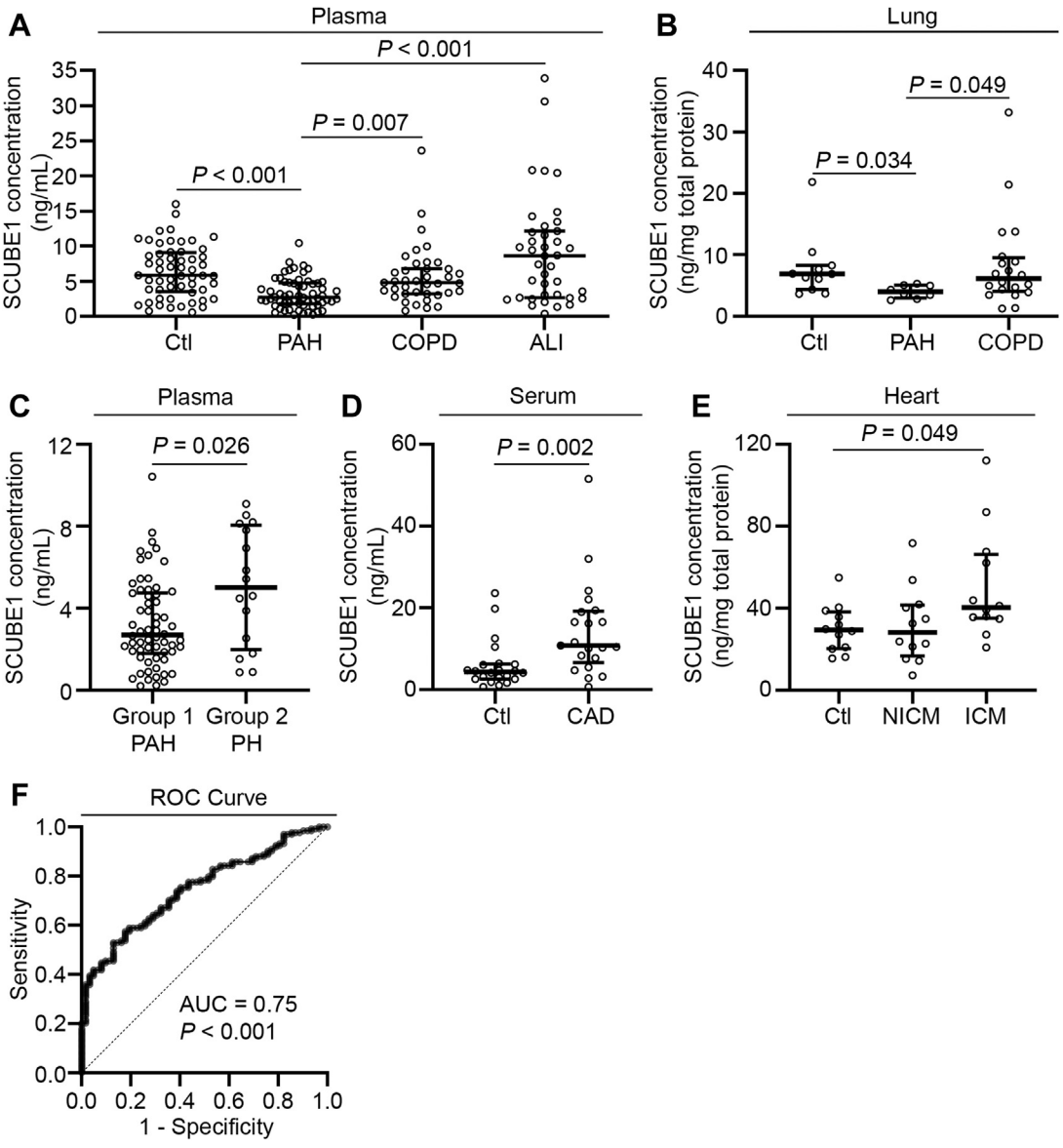

(A) Plasma was collected from the pulmonary arteries of patients with World Symposium on Pulmonary Hypertension (WSPH) group 1 (n = 62) at the time of right heart catheterization. Peripheral plasma samples were collected from patients without PH (non-PH) (n = 56), patients with chronic obstructive pulmonary disease (COPD) (n = 39), and acute lung injury (ALI) (n = 39). SCUBE1 protein was quantified and compared across cohorts. **(B)** SCUBE1 protein was quantified in lung tissue obtained from rapid autopsy or lung transplant of individuals with WSPH group 1 PAH (n = 8), non-PH (n = 11), or COPD (n = 20). **(C)** Plasma was collected from group 2 PH (n = 16), and SCUBE1 protein levels were compared with group 1 PAH plasma samples. **(D)** SCUBE1 protein was quantified in serum samples collected from patients with coronary angiogram–confirmed coronary artery disease (CAD) (n = 22) and non-CAD control subjects (n = 21). **(E)** SCUBE1 protein was quantified in myocardium tissue homogenates obtained from rapid autopsy or heart transplant of nondiseased individuals (Ctl) (n = 12), patients with nonischemic cardiomyopathy (NICM) (n = 12) and ischemic cardiomyopathy (ICM) (n = 12). **(F)** Receiver-operating characteristic (ROC) curve for sensitivity and specificity analysis between PAH and a combined non-PAH cohort composed of control, COPD, and ALI patients (Clopper-Pearson method). Grouped data are presented as medians with interquartile range. The p values were calculated by Mann-Whitney *U* tests for pairwise comparisons, and Kruskal-Wallis test with post hoc Dunn Multiple Comparison test. The comparisons with $p > 0.05$ were not explicitly stated in the panels. AUC = area under the curve; other abbreviations as in Figures 1 and 5.

(see Supplemental Table S7 for summary of statistics). Furthermore, the diagnostic OR, a single indicator of diagnostic performance, was calculated as previously described (28). The diagnostic OR for a plasma SCUBE1 cutpoint of 5.46 ng/ml was 7.6 (95% confidence interval: 3.4 to 16.9; $p < 0.001$) to diagnose PAH against non-PAH control subjects. We also performed a ROC analysis between group 1 PAH and group 2 PH cohorts, resulting in an AUC of 0.68 ($p = 0.027$). To discriminate between these PH subtypes, an optimal plasma SCUBE1 cutpoint of 5.01 ng/ml was defined, again with a high specificity of 0.82 and a sensitivity of 0.50 (see Supplemental Table S8 for summary of statistics). The diagnostic OR for this plasma SCUBE1 cutpoint was 4.6 (95% confidence interval: 1.5 to 14.7; $p = 0.011$) to diagnose group 1 PAH against group 2 PH.

THE DECREASE OF PLASMA SCUBE1 LEVELS CORRELATE WITH SEVERITY AND PROGRESSION OF PAH. We sought to determine whether SCUBE1 expression is correlated with hemodynamic or echocardiographic parameters linked to severity of PH. In patients with PAH, plasma SCUBE1 levels were found to be progressively reduced with increasing levels of either mPAP or PVR, with statistical significance in both regression analysis (**Figures 7A and 7C**) and the trend of decrease analysis when mPAP and PVR were binned into quartiles (**Figures 7B and 7D**). No correlation was observed between PCWP or cardiac output with plasma SCUBE1 levels (Supplemental Figure S3). When examining the UPMC cohort of patients, plasma SCUBE1 levels were also significantly lower in PAH patients with echocardiographic indices of severe PAH, including RV hypertrophy, moderate-to-severe RV dilation, or decreased tricuspid annular plane systolic excursion, a quantitative echocardiographic measurement reflecting RV dysfunction (**Figures 7E to 7G**).

DISCUSSION

To date, the complete molecular mechanisms that predispose persons carrying BMPR2 heterozygous mutations to PAH are not entirely defined, but iPSC technologies now allow for more direct investigation of BMPR2 deficiency in patients with predisposing mutations. By analyzing a publicly available RNA-sequencing dataset generated from iPSC-ECs of BMPR2-mutant carriers and PAH patients, SCUBE1 was identified as a BMPR2-relevant secreted factor regulated by multiple triggers of PAH and that modulates crucial endothelial pathophenotypes in PAH. Correspondingly, in multiple rodent models and patients with PAH, SCUBE1 levels were decreased and negatively correlated with the severity and progression of disease, suggesting the potential of developing SCUBE1 as a diagnostic and prognostic marker for this historically neglected disease.

In the past 2 decades, genomic and mechanistic studies have defined BMPR2 biology as a genetic (33) and molecular (34-36) lynchpin of PAH pathogenesis, but substantial knowledge gaps still exist. Pathogenic *BMPR2* mutations are genetically diverse (37) but produce a common haploinsufficiency that has been generally accepted as a driver of endothelial dysfunction, vascular remodeling, and vasoconstriction ultimately leading to clinical PAH (3). Although inherited in an autosomally dominant fashion, the incomplete penetrance of roughly 20% in families harboring pathogenic *BMPR2* mutations reveals our limited understanding of the complex genetic and environmental interactions behind its clinical manifestation (38). Part of our knowledge deficiency regarding BMPR2 biology can be attributed to the difficulty of recapitulating its haploinsufficiency using traditional knockdown experiments. Gu et al. (10) sought to bypass this obstacle by harnessing iPSC technology in which they performed RNA-sequencing on transcripts isolated from iPSC-ECs derived from PAH patients with *BMPR2* mutations, unaffected carriers of *BMPR2* mutations, and healthy control subjects. Rapid advances in analytical methods over the past several years, notably correction for G-C content (39), allowed us to reinterrogate their data with improved sensitivity for detecting differentially expressed genes at a comparable false discovery rate (15).

Whereas we focused our current investigation on SCUBE1, our RNA-sequencing analysis also identified 16 other genes that were differentially expressed between iPSC-ECs from BMPR2 mutants versus control subjects. Most differentially expressed transcripts were messenger RNAs, with a notable long noncoding RNA, H19, that has been recently connected to PAH pathogenesis (40,41). Furthermore, other genes have been linked to the interferon response, including *BST2* (42), *IFIT1*, *IFI6*, *IFI44L*, and *MX1* (29). Clinical reports of PAH onset after interferon therapy in diseases such as hepatitis C and multiple sclerosis have suggested that interferons may play a role in PAH pathogenesis, although preclinical studies have yielded conflicting results as to whether type I interferons play a therapeutic (43) or pathogenic (44) role in PAH. Although it is possible that distinct interferon-related profiles may represent artifacts of the iPSC-EC differentiation process (45,46), a recent study (29) linked MX1 to BMP signaling, providing internal validation of our approach and suggesting that the interaction of

FIGURE 7 Plasma SCUBE1 Levels Are Inversely Correlated With Disease Severity in Patients with WSPH Group 1 PAH

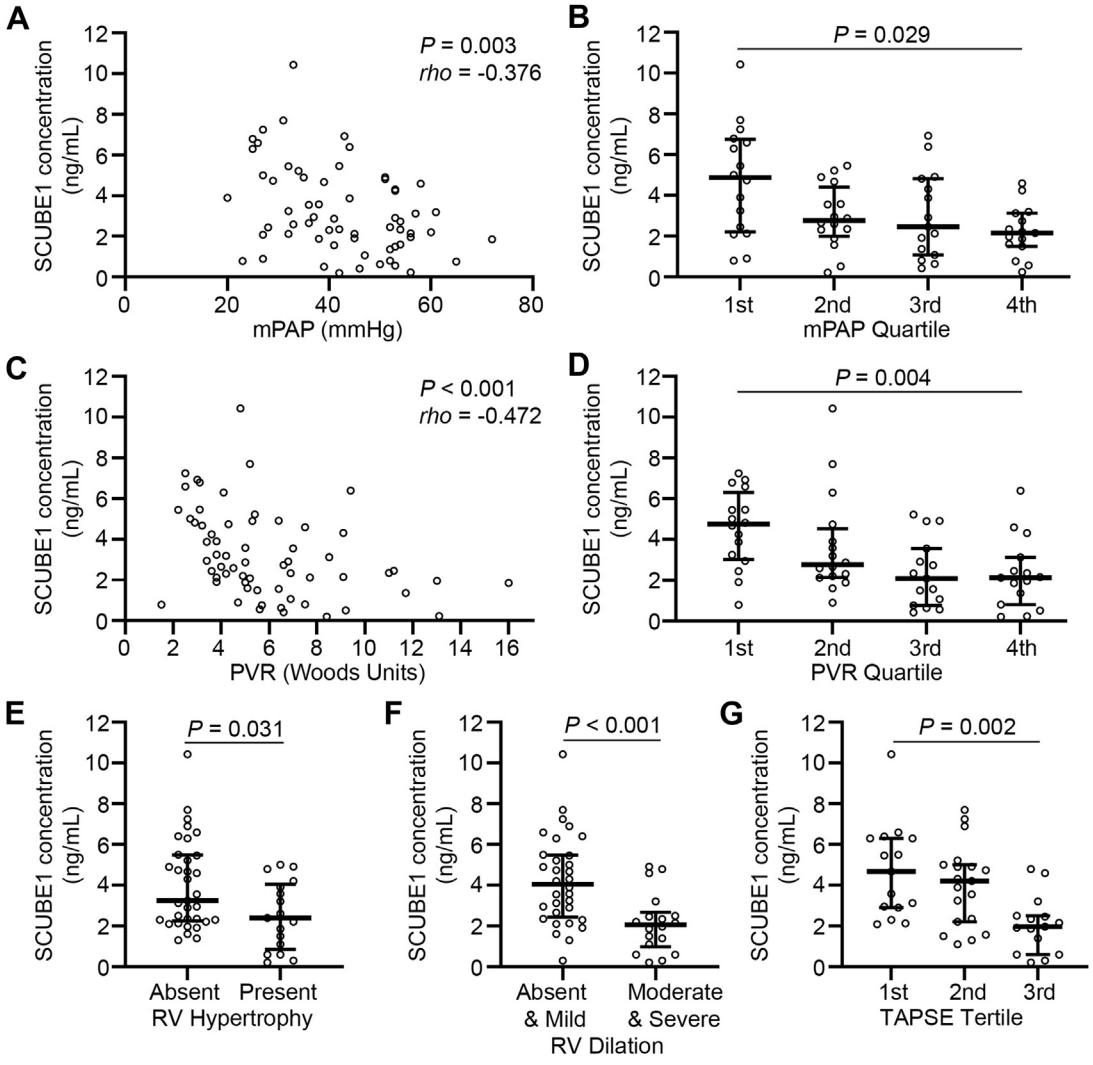

Plasma SCUBE1 concentration was compared across WSPH group 1 PAH patients with overall mean pulmonary artery pressure (mPAP) and calculated pulmonary vascular resistance (PVR) with Spearman correlation **(A,C)** or trend of change analysis in quartiles (binned based on minimum, 25th percentile, median, 75th percentile, and maximum) of mPAP (first quartile: 15 to 35 mm Hg; second quartile: 36 to 44 mm Hg; third quartile: 45 to 51 mm Hg; fourth quartile: 52 to 86 mm Hg) **(B)**, or PVR (first quartile: 1.30 to 4.06 Wood units [WU]; second quartile: 4.07 to 5.31 WU; third quartile: 5.32 to 8.42 WU; fourth quartile: 8.42 to 20.0 WU) **(D)**. **(E to G)** Transthoracic echocardiography images from the patient cohort managed at University of Pittsburgh Medical Center with WSPH group 1 PAH (n = 49 patients) were reviewed, and right ventricular (RV) dimensions and tricuspid annular plane systolic excursion (TAPSE) were directly measured from original transthoracic echocardiography images. Plasma SCUBE1 levels were compared within the population based on the degree of RV hypertrophy **(E)**, RV dilation **(F)**, or TAPSE tertile (binned based on minimum, 33th percentile, 66th percentile, and maximum. First quartile: 2.3 to 2.8 cm; second quartile: 1.7 to 2.3 cm; third quartile: 1.2 to 1.6 cm) **(G).** Grouped data are presented as median with interquartile range. The p values were calculated by Mann-Whitney *U* tests for pairwise comparisons, Kruskal-Wallis test for the change across quartiles and tertiles, and Spearman correlation analysis (*rho*: correlation coefficient). Abbreviations as in Figures 1 and 6.

interferon-associated signaling pathways with BMP in PAH is deserving of additional investigation.

The functional and structural interconnections of SCUBE1 and BMPR2 offer substantial insights into the molecular pathobiology of both of these molecules. SCUBE1 is a secreted and cell-surface protein that consists structurally of an NH2-terminal signal peptide sequence, an EGF-like repeat domain, a spacer

region, cysteine-rich motifs, and a COOH-terminal CUB (complement protein C1r/C1s, Uegf, and BMP1) domain, where expression is restricted mainly to platelets and endothelium during adulthood (11,30,47). In the current study, SCUBE1 deficiency recapitulated phenotypes associated with BMPR2 deficiency, including decreased angiogenic potential and increased apoptosis (48,49). Meanwhile, SCUBE1 overexpression displayed converse effects and reversed the phenotypes associated with multiple known PAH triggers in vitro. Interestingly, there is evidence that SCUBE1 may act as coactivator or interactor to both TGF-β receptor and BMPR2 (50); and the functional status and balance of these 2 cell-signaling systems are known to be critical in control of endothelial function in PAH (51). By examining BMPR2 and TGF-β receptor-specific SMADs, our data indicate that SCUBE1 preferentially controls SMADs more relevant to BMPR2 rather than to TGF-β (**Figure 4**). Considering our finding that BMPR2 knockdown can also down-regulate SCUBE1 (**Figure 1**), our findings support a model whereby SCUBE1 and BMPR2 form a positive feedback loop whereby deficiency of either of the 2 partners may transform the loop into a vicious cycle to further down-regulate the overall BMPR2 functional status in endothelial cells. Conversely, the enhancement of either SCUBE1 or BMPR2 could result in augmented functional regulation due to positive feedback to each other. This hypothesis endorses a potential to utilize SCUBE1 as a therapeutic target to effectively reinstall or augment BMPR2 signaling-related endothelial function during initiation and/or development of PAH.

Beyond BMPR2 deficiency, hypoxia and inflammatory factor IL-1β, 2 commonly recognized acquired triggering factors for PAH, also down-regulated SCUBE1 (**Figure 1**) with substantial dependence on HIF1A (**Figure 2**). Notably, HIF1A likely employs an indirect mechanism for down-regulation, given the lack of any known HIF1A binding consensus motif ([A/G]CGTG) (52) in the SCUBE1 promoter region (data not shown). Furthermore, at baseline, HIF1A siRNA knockdown did not alter BMPR2 expression and exerted no reversal effect on the down-regulation of SCUBE1 by BMPR2 siRNA. Thus, a HIF1A-independent mechanism must also exist, relevant to BMPR2-dependent effects on SCUBE1.

Our findings of circulating SCUBE1 plasma levels in patients with PAH that inversely correlate with disease severity emphasize the putative diagnostic and/or prognostic utility of this molecule. Owing to its role in platelet aggregation and thrombosis (11,13,53), SCUBE1 has been proposed as a plasma biomarker for myocardial infarction, thrombotic stroke, and pulmonary embolism (12,14). In the present study, we extensively tested the change of SCUBE1 levels in multiple acute and chronic cardiopulmonary pathologies, including pneumonia, ALI or acute respiratory distress syndrome, acute myocardial infarction, COPD, chronic stable CAD, ICM, and NICM. Importantly, in these other cardiopulmonary diseases, increased, rather than decreased, plasma SCUBE1 was associated with disease state, thus offering substantial specificity of our findings to PAH. This was reflected by the ROC analysis as well as a high specificity of 0.87 and a significant diagnostic OR of 7.6 at the optimal plasma SCUBE1 cutpoint of 5.46 ng/ml. These findings support the notion that decreased plasma SCUBE1 is effective in distinguishing the presence of PAH over benign contexts and other non-PAH cardiopulmonary conditions. The great need for a diagnostic and prognostic biomarker in PAH is highlighted by the fact that clinical symptoms often manifest late in the course of the disease when right heart failure is evident, thus delaying medical therapy (5). Meanwhile, survival times from PAH diagnosis have more than doubled since the advent of advanced therapies (54,55), suggesting that more expeditious application of these regimens could yield additional improvements in mortality. To date, however, the majority of candidate biomarkers have focused on nonspecific indicators of RV failure, angiogenesis, or inflammation (7). Recently, the identification of BMP9 as a clinical biomarker for portopulmonary hypertension emphasized the need for mechanistic biomarkers reflective of the underlying, and potentially genetic, pathophysiology (6). Whereas prior work has shown that plasma levels of soluble endoglin, a coreceptor involved in BMP signaling, are elevated in PAH and predict functional class (56), these measurements have not been shown to correlate with hemodynamic parameters. In contrast, our study found that plasma SCUBE1 levels are tightly and negatively correlated with mPAPs and PVR as well as indices of RV dysfunction. It remains to be seen whether SCUBE1 similarly correlates with functional workload indices, such as 6-min walk test or $V_{O_{2max}}$. Additionally, future studies should plan to follow SCUBE1 levels over time to determine whether they track with early disease onset, disease progression, and recovery with treatment.

Our work also suggests a diagnostic value of SCUBE1 for differentiating WSPH group 1 PAH from group 2 PH. Often, group 2 PH can clinically masquerade as group 1 PAH, particularly after diuresis. As such, inappropriate pulmonary vasodilator treatment may be considered for group 2 PH patients when diagnostic criteria are blurred (57).

The decreased SCUBE1 levels observed in group 1 PAH, but not group 2 PH, in this initial study begin to clarify the distinct pathogenetic features between these 2 clinical groups. In this context, we acknowledge that the discriminatory performance of SCUBE1 levels was modest (AUC: 0.68) and was likely driven by the known heterogeneity across group 2 PH patients and particularly by the wide range of PVR. Future studies of SCUBE1 plasma levels across group 2 PH subtypes could offer important data to optimize the discriminatory potential of this marker even further. Finally, beyond these PH groups, additional studies examining the association of plasma SCUBE1 levels with WSPH group 3 (PH related to lung disease and hypoxia) and group 4 PH (chronic thromboembolic PH), will be of great interest, given the potential for platelet-released SCUBE1 to contribute to the directional gradient of our proposed biomarker.

STUDY LIMITATIONS. First, whereas forced SCUBE1 expression appears to reverse pathophenotypes associated with BMPR2-deficiency in vitro, further work is needed to determine the therapeutic potential of SCUBE1 in vivo. Second, although our present study focused on SCUBE1 deficiency in endothelium, platelets are a known source of SCUBE1 and their contribution to our in vivo observations warrants further investigation in future work. Third, the sensitivity and specificity of plasma SCUBE1 level as a diagnostic marker were evaluated retrospectively in a relatively small sample size. A clinical study with prospective and increased enrollment should be planned for further validation and statistical analysis.

CONCLUSIONS

In summary, guided by RNA-sequencing in iPSC-ECs from PAH patients, we identified SCUBE1 as a novel pathogenic factor regulating pulmonary endothelial pathophenotypes through its control of BMPR2-relevant SMAD signaling. SCUBE1 levels are inversely correlated with the severity and progression of disease in PAH, suggesting the value of developing SCUBE1 as a clinical BMPR2-relevant marker for diagnosis and prognosis of disease.

ACKNOWLEDGMENTS The authors acknowledge the Center for Organ Recovery and Education, the organ donors, and their families for human lung and heart tissue samples used in this study.

AUTHOR DISCLOSURES

This work was supported by National Institutes of Health grants R01 HL124021, HL 122596, HL 138437, and UH2 TR002073 (to Dr. Chan); 2P01 HL103455 and 1R01AG058659 (to Dr. Simon); HL142084 and HL136143 (to Dr. Lee); R00HL121076-03, R01HL143967, and R01HL142629 (to Dr. Dutta); and 5T32HL129964-04 (to Dr. Sun). This work was also supported by American Heart Association Established Investigator Award 18EIA33900027 (to Dr. Chan), as well as Texas A and M University Systems Chancellors' Research Initiative for Center for Computational Systems Biology at Prairie View A and M University (to Dr. Kim). Drs. Sun and Chan filed patent applications regarding the targeting of bone morphogenetic protein signaling in pulmonary hypertension. Dr. Simon has received research grants from Novartis and Aadi; and has received consulting fees from Complexa, United Therapeutics, and Actelion. Dr. Mazurek has served as a consultant for United Therapeutics and Actelion; and has received research support from Tenax Therapeutics, Complexa Inc., and Actelion. Dr. Vaidya has served as a consultant for Bayer, Actelion, and United Therapeutics. Dr. Chan has served as a consultant for Zogenix, Aerpio, and United Therapeutics; is a director, officer, and shareholder in Numa Therapeutics; and has held research grants from Actelion and Pfizer. All other authors have reported that they have no relationships relevant to the contents of this paper to disclose.

ADDRESS FOR CORRESPONDENCE: Dr. Stephen Y. Chan, Center for Pulmonary Vascular Biology and Medicine, Pittsburgh Heart, Lung, and Blood Vascular Medicine Institute, Division of Cardiology, Department of Medicine, University of Pittsburgh Medical Center, 200 Lothrop Street, BST1704.2, Pittsburgh, Pennsylvania 15261. E-mail: chansy@pitt.edu.

PERSPECTIVES

COMPETENCY IN MEDICAL KNOWLEDGE: PAH has long been associated with genetic BMPR2 haploinsufficiency, but the molecular intermediaries between genetic susceptibility and disease pathogenesis remain ill-defined. Prompt identification and treatment of PAH patients is hindered by the unreliability of proposed biomarkers that have historically been indicators of disease effects rather than primary mechanisms. This study identified SCUBE1 as a novel BMPR2-associated mediator of endothelial pathophenotypes with potential utility as a mechanistic biomarker in PAH. Clinically, SCUBE1 levels correlate with indices of disease severity and serve as highly specific diagnostic markers that could distinguish PAH from benign contexts or other cardiopulmonary conditions.

TRANSLATIONAL OUTLOOK: Additional preclinical in vivo studies are needed to further define the role of SCUBE1 in PAH pathogenesis and its therapeutic utility, whereas clinical studies with longitudinal prospective patient data will be required to further determine the diagnostic and prognostic efficacy of SCUBE1 as a biomarker for PAH.

REFERENCES

1. Simonneau G, Montani D, Celermajer DS, et al. Haemodynamic definitions and updated clinical classification of pulmonary hypertension. Eur Respir J 2019;53:1801913.

2. Rabinovitch M. Molecular pathogenesis of pulmonary arterial hypertension. J Clin Invest 2012;122:4306–13.

3. Machado RD, Pauciulo MW, Thomson JR, et al. BMPR2 haploinsufficiency as the inherited molecular mechanism for primary pulmonary hypertension. Am J Hum Genet 2001;68:92–102.

4. Farber HW, Miller DP, Poms AD, et al. Five-year outcomes of patients enrolled in the REVEAL Registry. Chest 2015;148:1043–54.

5. Brown LM, Chen H, Halpern S, et al. Delay in recognition of pulmonary arterial hypertension: factors identified from the REVEAL Registry. Chest 2011;140:19–26.

6. Nikolic I, Yung LM, Yang P, et al. Bone morphogenetic protein 9 is a mechanistic biomarker of portopulmonary hypertension. Am J Respir Crit Care Med 2019;199:891–902.

7. Anwar A, Ruffenach G, Mahajan A, Eghbali M, Umar S. Novel biomarkers for pulmonary arterial hypertension. Respir Res 2016;17:88.

8. de Jesus Perez VA, Alastalo TP, Wu JC, et al. Bone morphogenetic protein 2 induces pulmonary angiogenesis via Wnt-beta-catenin and Wnt-RhoA-Rac1 pathways. J Cell Biol 2009;184:83–99.

9. Teichert-Kuliszewska K, Kutryk MJ, Kuliszewski MA, et al. Bone morphogenetic protein receptor-2 signaling promotes pulmonary arterial endothelial cell survival: implications for loss-of-function mutations in the pathogenesis of pulmonary hypertension. Circ Res 2006;98:209–17.

10. Gu M, Shao NY, Sa S, et al. Patient-specific iPSC-derived endothelial cells uncover pathways that protect against pulmonary hypertension in BMPR2 mutation carriers. Cell Stem Cell 2017;20:490–504.

11. Tu CF, Yan YT, Wu SY, et al. Domain and functional analysis of a novel platelet-endothelial cell surface protein, SCUBE1. J Biol Chem 2008;283:12478–88.

12. Dai DF, Thajeb P, Tu CF, et al. Plasma concentration of SCUBE1, a novel platelet protein, is elevated in patients with acute coronary syndrome and ischemic stroke. J Am Coll Cardiol 2008;51:2173–80.

13. Wu MY, Lin YC, Liao WJ, et al. Inhibition of the plasma SCUBE1, a novel platelet adhesive protein, protects mice against thrombosis. Arterioscler Thromb Vasc Biol 2014;34:1390–8.

14. Turkmen S, Sahin A, Gunaydin M, et al. The value of signal peptide-CUB-EGF domain-containing protein-1 (SCUBE1) in the diagnosis of pulmonary embolism: a preliminary study. Acad Emerg Med 2015;22:922–6.

15. Patro R, Duggal G, Love MI, Irizarry RA, Kingsford C. Salmon provides fast and bias-aware quantification of transcript expression. Nat Methods 2017;14:417–9.

16. Bioconductor. Open Source Software for Bioinformatics. Available at: http://bioconductor.org/. Accessed September 24, 2020.

17. Soneson C, Love MI, Robinson MD. Differential analyses for RNA-seq: transcript-level estimates improve gene-level inferences. F1000Res 2015;4:1521.

18. Love MI, Huber W, Anders S. Moderated estimation of fold change and dispersion for RNA-seq data with DESeq2. Genome Biol 2014;15:550.

19. Yu Q, Tai YY, Tang Y, et al. BOLA (BolA family member 3) deficiency controls endothelial metabolism and glycine homeostasis in pulmonary hypertension. Circulation 2019;139:2238–55.

20. Olonisakin TF, Li H, Xiong Z, et al. CD36 provides host protection against *Klebsiella pneumoniae* intrapulmonary infection by enhancing lipopolysaccharide responsiveness and macrophage phagocytosis. J Infect Dis 2016;214:1865–75.

21. Dutta P, Courties G, Wei Y, et al. Myocardial infarction accelerates atherosclerosis. Nature 2012;487:325–9.

22. ARDS Definition Task Force, Ranieri VM, Rubenfeld GD, et al. Acute respiratory distress syndrome: the Berlin definition. JAMA 2012;307:2526–33.

23. Simonneau G, Gatzoulis MA, Adatia I, et al. Updated clinical classification of pulmonary hypertension. J Am Coll Cardiol 2013;62 Suppl 25:D34–41.

24. Rudski LG, Lai WW, Afilalo J, et al. Guidelines for the echocardiographic assessment of the right heart in adults: a report from the American Society of Echocardiography endorsed by the European Association of Echocardiography, a registered branch of the European Society of Cardiology, and the Canadian Society of Echocardiography. J Am Soc Echocardiogr 2010;23:685–713.

25. DeLong ER, DeLong DM, Clarke-Pearson DL. Comparing the areas under two or more correlated receiver operating characteristic curves: a nonparametric approach. Biometrics 1988;44:837–45.

26. Clopper CJ, Pearson ES. The use of confidence or fiducial limits illustrated in the case of the binomial. Biometrika 1934;26:404–13.

27. Youden WJ. Index for rating diagnostic tests. Cancer 1950;3:32–5.

28. Glas AS, Lijmer JG, Prins MH, Bonsel GJ, Bossuyt PM. The diagnostic odds ratio: a single indicator of test performance. J Clin Epidemiol 2003;56:1129–35.

29. Yuan H, Sehgal PB. MxA is a novel regulator of endosome-associated transcriptional signaling by bone morphogenetic proteins 4 and 9 (BMP4 and BMP9). PLoS One 2016;11:e0166382.

30. Yang RB, Ng CK, Wasserman SM, et al. Identification of a novel family of cell-surface proteins expressed in human vascular endothelium. J Biol Chem 2002;277:46364–73.

31. Sancisi V, Gandolfi G, Ragazzi M, et al. Cadherin 6 is a new RUNX2 target in TGF-beta signalling pathway. PLoS One 2013;8:e75489.

32. Jung YJ, Isaacs JS, Lee S, Trepel J, Neckers L. IL-1beta-mediated up-regulation of HIF-1alpha via an NFkappaB/COX-2 pathway identifies HIF-1 as a critical link between inflammation and oncogenesis. FASEB J 2003;17:2115–7.

33. Machado RD, Eickelberg O, Elliott CG, et al. Genetics and genomics of pulmonary arterial hypertension. J Am Coll Cardiol 2009;54 Suppl 1:S32–42.

34. Johnson DW, Berg JN, Baldwin MA, et al. Mutations in the activin receptor-like kinase 1 gene in hereditary haemorrhagic telangiectasia type 2. Nat Genet 1996;13:189–95.

35. McAllister KA, Grogg KM, Johnson DW, et al. Endoglin, a TGF-beta binding protein of endothelial cells, is the gene for hereditary haemorrhagic telangiectasia type 1. Nat Genet 1994;8:345–51.

36. Shintani M, Yagi H, Nakayama T, Saji T, Matsuoka R. A new nonsense mutation of SMAD8 associated with pulmonary arterial hypertension. J Med Genet 2009;46:331–7.

37. Austin ED, Loyd JE. The genetics of pulmonary arterial hypertension. Circ Res 2014;115:189–202.

38. Larkin EK, Newman JH, Austin ED, et al. Longitudinal analysis casts doubt on the presence of genetic anticipation in heritable pulmonary arterial hypertension. Am J Respir Crit Care Med 2012;186:892–6.

39. Love MI, Hogenesch JB, Irizarry RA. Modeling of RNA-seq fragment sequence bias reduces systematic errors in transcript abundance estimation. Nat Biotechnol 2016;34:1287–91.

40. Wang R, Zhou S, Wu P, et al. Identifying involvement of H19-miR-675-3p-IGF1R and H19-miR-200a-PDCD4 in treating pulmonary hypertension with melatonin. Mol Ther Nucleic Acids 2018;13:44–54.

41. Su H, Xu X, Yan C, et al. LncRNA H19 promotes the proliferation of pulmonary artery smooth muscle cells through AT1R via sponging let-7b in monocrotaline-induced pulmonary arterial hypertension. Respir Res 2018;19:254.

42. Blasius AL, Giurisato E, Cella M, Schreiber RD, Shaw AS, Colonna M. Bone marrow stromal cell antigen 2 is a specific marker of type I IFN-producing cells in the naive mouse, but a promiscuous cell surface antigen following IFN stimulation. J Immunol 2006;177:3260–5.

43. Bauer EM, Zheng H, Lotze MT, Bauer PM. Recombinant human interferon alpha 2b prevents and reverses experimental pulmonary hypertension. PLoS One 2014;9:e96720.

44. George PM, Oliver E, Dorfmuller P, et al. Evidence for the involvement of type I interferon in pulmonary arterial hypertension. Circ Res 2014;114:677–88.

45. Eggenberger J, Blanco-Melo D, Panis M, Brennand KJ, tenOever BR. Type I interferon

response impairs differentiation potential of pluripotent stem cells. Proc Natl Acad Sci U S A 2019;116:1384–93.

46. Khan KA, Do F, Marineau A, et al. Fine-tuning of the RIG-I-like receptor/interferon regulatory factor 3-dependent antiviral innate immune response by the glycogen synthase kinase 3/beta-catenin pathway. Mol Cell Biol 2015;35:3029–43.

47. Grimmond S, Larder R, Van Hateren N, et al. Cloning, mapping, and expression analysis of a gene encoding a novel mammalian EGF-related protein (SCUBE1). Genomics 2000;70:74–81.

48. Wang H, Ji R, Meng J, et al. Functional changes in pulmonary arterial endothelial cells associated with BMPR2 mutations. PLoS One 2014;9:e106703.

49. Sa S, Gu M, Chappell J, et al. Induced pluripotent stem cell model of pulmonary arterial hypertension reveals novel gene expression and patient specificity. Am J Respir Crit Care Med 2017;195:930–41.

50. Tsao KC, Tu CF, Lee SJ, Yang RB. Zebrafish scube1 (signal peptide-CUB (complement protein C1r/C1s, Uegf, and Bmp1)-EGF (epidermal growth factor) domain-containing protein 1) is involved in primitive hematopoiesis. J Biol Chem 2013;288:5017–26.

51. Rol N, Kurakula KB, Happe C, Bogaard HJ, Goumans MJ. TGF-beta and BMPR2 signaling in PAH: two black sheep in one family. Int J Mol Sci 2018;19:2585.

52. Kimura H, Weisz A, Ogura T, et al. Identification of hypoxia-inducible factor 1 ancillary sequence and its function in vascular endothelial growth factor gene induction by hypoxia and nitric oxide. J Biol Chem 2001;276:2292–8.

53. Tu CF, Su YH, Huang YN, et al. Localization and characterization of a novel secreted protein SCUBE1 in human platelets. Cardiovasc Res 2006;71:486–95.

54. D'Alonzo GE, Barst RJ, Ayres SM, et al. Survival in patients with primary pulmonary hypertension: results from a national prospective registry. Ann Intern Med 1991;115:343–9.

55. Benza RL, Miller DP, Barst RJ, Badesch DB, Frost AE, McGoon MD. An evaluation of long-term survival from time of diagnosis in pulmonary arterial hypertension from the REVEAL Registry. Chest 2012;142:448–56.

56. Malhotra R, Paskin-Flerlage S, Zamanian RT, et al. Circulating angiogenic modulatory factors predict survival and functional class in pulmonary arterial hypertension. Pulm Circ 2013;3:369–80.

57. Maron BA, Ryan JJ. A concerning trend for patients with pulmonary hypertension in the era of evidence-based medicine. Circulation 2019;139:1861–4.

KEY WORDS BMPR2, endothelium, pulmonary hypertension, SCUBE1

APPENDIX For supplemental figures and tables, please see the online version of this paper.